



Norwegian
Meteorological
Institute

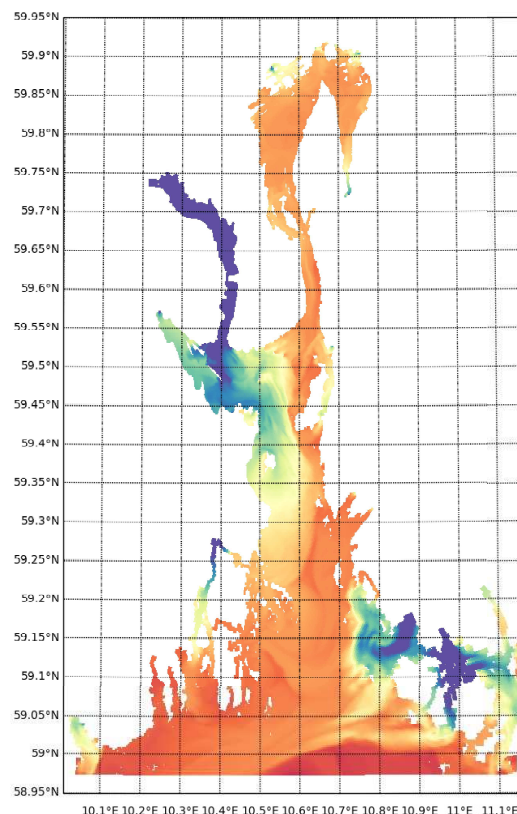
METreport

No. 4/2016
ISSN 2387-4201
Oceanography

A high-resolution, curvilinear ROMS model for the Oslofjord

FjordOs technical report No. 2

Lars Petter Røed^{1,2}, Nils Melsom Kristensen¹,
Karina Bakkeløkken Hjelmervik³ and André Staalstrøm⁴



HSN Høgskolen
i Sørøst-Norge



¹Norwegian Meteorological Institute, ²Department of Geosciences, University of Oslo,
³University College of Southeast Norway, ⁴Norwegian Institute of Water Research



Title A high-resolution, curvilinear ROMS model for the Oslofjord. FjordOs technical report No. 2	Date June 7, 2016
Section Ocean and Ice	Report no. 4/2016
Author(s) Lars Petter Røed, Nils Melsom Kristensen, Karina Bakkeløkken Hjelmervik, André Staalstrøm	Classification <input checked="" type="radio"/> Free <input type="radio"/> Restricted
Client(s) Oslofjordfondet	Client's reference
Abstract Provided is documentation of a new Oslofjord model, FjordOs CL, utilizing the curvilinear option of the Regional Ocean Modeling System - ROMS. The development is part of the project FjordOs. FjordOs CL has a spatial grid size varying from about 50 meters in the Drøbak sound to about 300 meters at its southern open boundary bordering on the Skagerrak. It features 42 terrain-following levels in the vertical. In addition to being forced by atmospheric, river and tidal input it is also forced by oceanic input at the open boundary. The atmospheric input is extracted from MET Norway's operational NWP model (AROME-MetCoOp), while oceanic input is extracted from MET Norway's operational, ocean forecasting model NorKyst800. The river input consists of observational based estimated discharges from 37 rivers along the perimeter of the fjord. The tidal input is based on the TPXO Atlantic database modified by observations and consists of nine tidal constituents as input.	
Keywords Ocean model, Numerical methods, Oslofjord, ROMS	

Disciplinary signature
Kai H. Christensen

iii

Responsible signature
Lars Anders Breivik

Abstract

Provided is documentation of a new Oslofjord model, FjordOs CL, utilizing the curvilinear option of the Regional Ocean Modeling System - ROMS. The development is part of the project FjordOs. FjordOs CL has a spatial grid size varying from about 50 meters in the Drøbak sound to about 300 meters at its southern open boundary bordering on the Skagerrak. It features 42 terrain-following levels in the vertical. In addition to being forced by atmospheric, river and tidal input it is also forced by oceanic input at the open boundary. The atmospheric input is extracted from MET Norway's operational NWP model (AROME-MetCoOp), while oceanic input is extracted from MET Norway's operational, ocean forecasting model NorKyst800. The river input consists of observational based estimated discharges from 37 rivers along the perimeter of the fjord. The tidal input is based on the TPXO Atlantic database modified by observations and consists of nine tidal constituents as input.

Contents

1	Introduction	1
1.1	The Oslofjord	1
1.2	Why a new model?	4
1.3	Organization of the report	8
2	The new model	9
2.1	Why ROMS?	10
2.2	The curvilinear FjordOs CL grid	10
3	Model specifics	13
4	Bathymetry and external forcing	15
4.1	Bathymetry	15
4.2	Atmospheric forcing	17
4.3	Input at open lateral boundaries	17
4.3.1	De-tided input	18
4.3.2	Tidal forcing	19
4.4	River input	21
5	Sample results	26
5.1	Currents	27
5.2	Hydrography and sea level	32
6	Summary and final remarks	36

List of Figures

Figure 1	The topography and irregular coastline of the Oslofjord and its location in Southern Norway. The right-hand gray scale bar indicates depth in meters. The blue arrow points to the location of the fjord’s main sill (the Drøbak sill as enlarged in Figure 2) which is only ~ 20 m deep. Note also the ~ 400 m deep basin extending from the Skagerrak towards the Hvaler Archipelago in the southeast, the so called Hvalerdjupet.	2
Figure 2	The irregular coastline and topography in the Drøbak Sill area.	3
Figure 3	The irregular coastline geometry and topography in the Færder National Park (left-hand panel) and the Hvaler National Park (right-hand panel). Note the many islands, narrow straits and channels present in these areas of the Oslofjord.	4
Figure 4	Map (left) showing the location where the ship “Godafoss” (right) grounded February 17, 2011. The location is in the sound Løperen between two of the major islands in the Hvaler Archipelago where Norway’s largest river flows through on its way to the Oslofjord.	5
Figure 5	The area covered by the NorKyst800 model. Shown is forecasted, 24 hour average speed at 3 m depth valid for February 22, 2016. Color bar gives speed in m/s with a a contour interval of 0.05 m/s.	6
Figure 6	Illustrated is the impact of grid resolution on how the Oslofjord is portrayed. Upper two panels show what the fjord looks like utilizing respectively a 20 km grid (left) and 4 km grid (right). Bottom panel show the same for utilizing a 800 m grid to represent the fjord. As revealed the smaller the grid size (higher grid resolution) the better the coastline geometry is represented.	7
Figure 7	The irregular coastline geometry and topography in the Oslofjord as portrayed in maps (left-hand panel) and the NorKyst800 model (right-hand panel). The red star sign marks the location of the Færder lighthouse. Note the difference in size and depth of the major Hvalerdjupet basin near the southern boundary and the general smoothness of the NorKyst800 topography compared to the real topography.	9
Figure 8	The FjordOs CL computational domain showing (a) the curvilinear grid configuration, and (b) the resulting grid resolution. The right-hand color bar indicates grid size in meters, while the left-hand bluescaled colorbar indicates depth in meters. X-axis is degrees east, and y-axis is degrees north.	11

Figure 9	The transformed curvilinear grid of the Oslofjord. The colors gives the depth in meters according to the color bar to the right. Model grid numbers associated with the curvilinear grid are given along the axes. There are 300 x 900 grid points.	12
Figure 10	The horizontal distribution and numbering system of variables in the ROMS grid. The figure is downloaded from the http://www.myroms.org website.	14
Figure 11	The vertical distribution and numbering system of variables in the ROMS grid. The figure is downloaded from the http://www.myroms.org website. . . .	15
Figure 12	Sketch of the vertical distribution of <i>s</i> -levels in the FjordOs CL model (cross-section at Breidangen, $y=600$).	16
Figure 13	The area covered by the Arome-MetCoop model. Shown is the forecasted (lead time 3 hrs) mean sea level pressure in hPa (black solid lines, countour interval = 5 hPa), 3 hourly precipitation, and 10 m wind valid at 1500UTC on February 22, 2016. Color bar indicates precipitation with a variable contour interval in the range 0.2-15 mm or larger (deep blue).	18
Figure 14	Left panel shows the many rivers (blue solid lines) emptying freshwater to the fjord (from NVE elvenett). The red numbers indicate a Main Catchment Area (MCA). The red dots indicate the location of the individual rivers discharging freshwater to Oslofjord (cf. Table 5). Some of the larger rivers, for instance Glomma, Drammenselva and Numedalslågen, are marked with a thicker blue line. Stations with water discharge measurements are shown with green dots and numbered with black numbers, e.g. q8. Right panel shows the location of the 37 rivers named in Table 5.	22
Figure 15	Currents at 2 meter depth for the inner part of the Oslofjord (ncluding Bunnefjorden and Oslo Harbour.	27
Figure 16	As Figure 15, but for the Drøbak Sound and Vestfjorden area.	28
Figure 17	As Figure 15, but for the Drammensfjord (left) and southern part of the Drøbak Sound and Breiangen area. Note the swift currents through narrow and shallow sound in the Svelvik area.	29
Figure 18	As Figure 15, but for the area between the Bastøy, Rauer and Bolærne islands.	30
Figure 19	As Figure 15, but for the area around the Færder lighthouse.	31
Figure 20	As Figure 21, but for sea surface salinity (SSS).	33

Figure 21 Sea surface temperature (SST) for the entire model domain of the Fjor-
dOs model. Note the high SST in the Drammensfjorden area. We believe this
is most likely caused by the entrainment (mixing) of warmer water from below.
This warm water is probably left from imperfect initial conditions. 34

Figure 22 As for figure 21, but for sea surface height (SSH). 35

List of Tables

Table 1	List of FjordOs CL model set-up parameters.	16
Table 2	List of atmospheric forcing parameters.	19
Table 3	Simulated tidal amplitudes [cm] and phases [deg] for a location close to the Viker tidal gauge station. The column "ATPXO" refers to the simulated tides using the TPXO Atlantic data base as input, while the column "Modified" refers to a run using adjusted tides as input. The column "Observed" refers to the observed tides at the nearby Viker tidal gauge station and is added for comparison.	20
Table 4	As Table 3, but for the Oscarsborg tidal gauge station.	21
Table 5	Rivers in the FjordOs CL model. The outlet positions follow the index convention in ROMS. The position is at a u -point if the direction is along the x -axis, and at a v -point if the direction is along the y -axis. The index counting in ROMS starts at 0, except for the u -points and v -points, where the count starts at 1. MCA: Main Catchment Area.	23
Table 6	Estimating discharges in unobserved MCAs based on observations at four MCAs with observations using the least mean square fit (9).	26

1 Introduction

Provided is a documentation of a new and recently developed Oslofjord model called FjordOs CL. FjordOs CL is based on version 3.6 of the Regional Ocean Modeling System - ROMS (*Haidvogel et al.*, 2008; *Shchepetkin and McWilliams*, 2005, 2009) utilizing its curvilinear option. The model is developed as part of the project "New Oslofjord model for prediction of currents, water level and hydrography, here applied on oil spill preparedness and harbor development - FjordOs"¹. FjordOs is a cooperation between MET Norway, University College of South-East Norway (HSN), The Norwegian Institute for Water Research (NIVA), The Norwegian Coastal Administration (Kystverket), Exxonmobil, Norwegian Defence Research Establishment (FFI), Vestfold, Buskerud and Østfold county and AGNES AB Miljøkonsulent.

1.1 The Oslofjord

The Oslofjord is located in Southern Norway and is about 100 km long (Figure 1). Its width varies from about 25 km at the entrance ($\sim 59^\circ\text{N}$) to about 1-2 km in the Drøbak Sound and Drøbak area. The fjord's main sill, which is marked by the blue arrow in Figure 1 (hereafter the Drøbak Sill), is located two thirds inside of the entrance to the fjord. This makes the Oslofjord peculiar among Norwegian fjords in that most of them have the sill at the entrance to the fjord.

The Drøbak Sill is partly man made² and partly natural. The natural sill is about 20 m deep, while the man made part is only 1-2 m deep. The latter consists of an underwater barrier, the Drøbak Jetty, extending halfway across the Drøbak Sound from the western mainland south of Drøbak to south of the small island Kaholmen located slightly to the east of the southern tip of the Håøya Island (Figure 2). There are two narrow openings in the Jetty with a maximum depth of about 6 m. One is located close to the mainland on the western side, while the second runs east-west and is located just south of Kaholmen.

The sill area represent a major obstruction for the water exchange between the inner and the outer part of the fjord. Due its narrowness and shallowness the Drøbak Sill area is famous for its strong tidal currents that easily exceeds 1 m/s. We also note that north of the sill the fjord is separated by Håøya Island into an eastern and a western channel each

¹<http://www.fjordos.no>

²The jetty was built in the years 1874 - 1879 as a naval defense of Oslo, the capital of Norway. It forces large vessels to sail east of the fortress Oscarsborg built at Kaholmen.

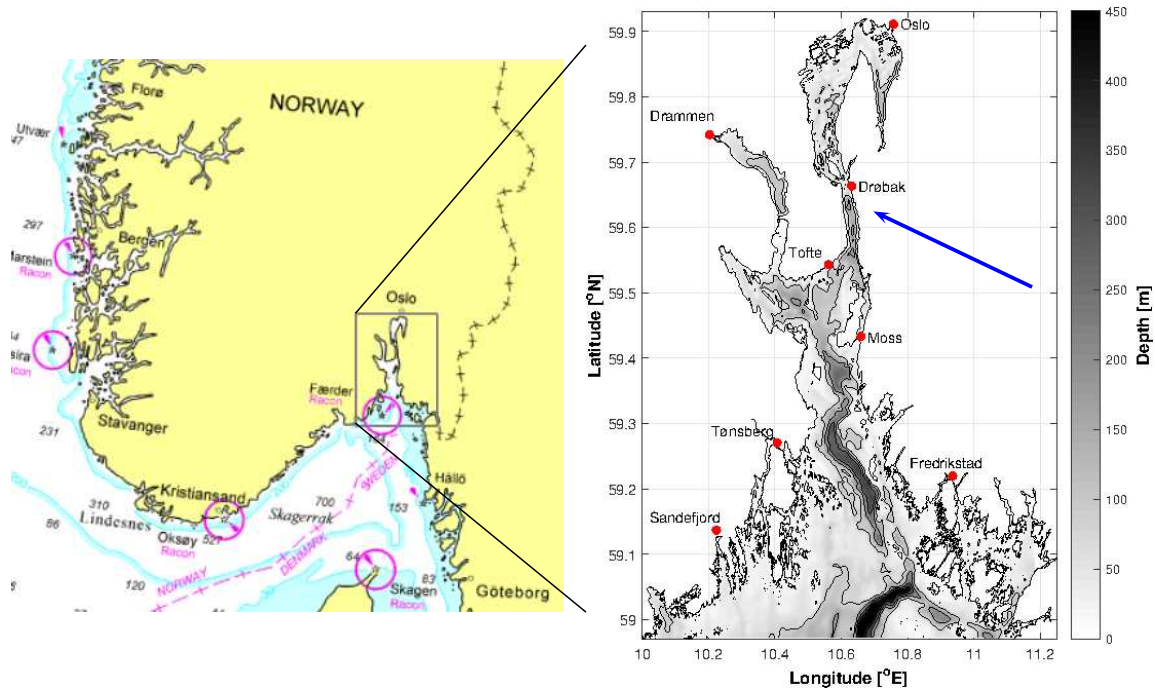


Figure 1: The topography and irregular coastline of the Oslofjord and its location in Southern Norway. The right-hand gray scale bar indicates depth in meters. The blue arrow points to the location of the fjord's main sill (the Drøbak sill as enlarged in Figure 2) which is only ~ 20 m deep. Note also the ~ 400 m deep basin extending from the Skagerrak towards the Hvaler Archipelago in the southeast, the so called Hvalerdjupet.

about 1 km wide. These channels and the openings in the Jetty are important to include in any model of the Oslofjord to obtain realistic circulation patterns and strengths in the area. Another noteworthy topographic feature is the Hvalerdjupet located at the entrance to the fjord (Figures 1 and 3). It is a 400 m deep basin extending northeastward from the Skagerrak towards the Hvaler Archipelago. As revealed by Figure 1 there are also several other somewhat shallower basins $\sim 150 - 200$ m deep as we proceed into the fjord.

In addition to the Drøbak Sill area there are other areas in the fjord that features many smaller and larger islands. For instance to the west we find the Tønsberg Archipelago including Bolærne, Store and Lille Færder (Færder Lighthouse), and to the east we find Rauer and Hankø, the Hvaler Archipelago and the smaller Islands Søstrene and Misingene (Figure 3). Further north on the west side of the fjord we find Bastø south of Horten, and to the east Jeløya. Jeløya is separated from the mainland by a narrow channel about 50 m wide within which water sloshes back and forth with the tides (*Hjelmervik et al.*,

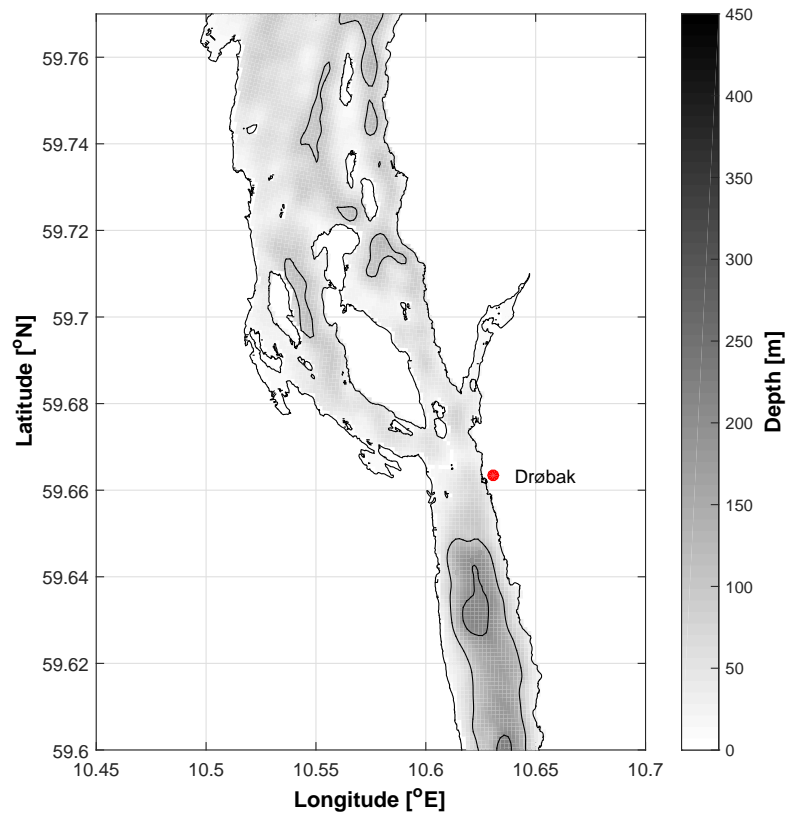


Figure 2: The irregular coastline and topography in the Drøbak Sill area.

2014). The presence of these archipelagos with its small islands give rise to many narrow sounds, straits and channels impeding the water exchange. If the goal is to compute realistic pathways of any unwanted substances discharged to the fjord or trajectories of floating structures including man overboard (Search and Rescue Services), we need to resolve, to the best of our ability, these features.

Finally it is worth mentioning the many rivers discharge freshwater to the fjord. For instance two of Norway’s largest rivers, namely Glomma and Drammenselva³, are emptying their freshwater into the Oslofjord with a mean discharge of 729 and 317 m³/s, respectively (*Milliman and Farnsworth, 2011*). This freshwater has a decisive impact on the salinity and hence on the circulation in the fjord. Furthermore, in most fjords the

³Here it is chosen to use Norwegian river names in which “elv” or “vassdrag”, means “river” or “water course”.

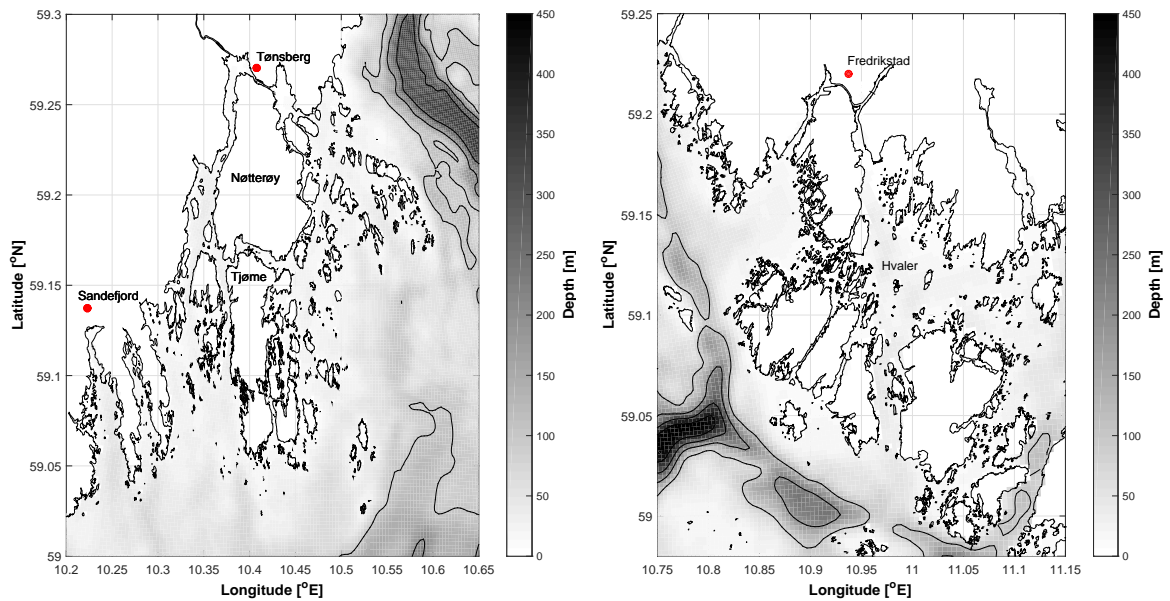


Figure 3: The irregular coastline geometry and topography in the Færder National Park (left-hand panel) and the Hvaler National Park (right-hand panel). Note the many islands, narrow straits and channels present in these areas of the Oslofjord.

river outlet is located at the fjord head leading to an estuarine circulation. In contrast the Glomma outlet is located in the outer part of the Oslofjord within the Hvaler Archipelago, while the Drammenselva outlet is located in the middle part of the fjord. As a result the estuarine circulation in the Oslofjord deviates considerably from a classical textbook example.

1.2 Why a new model?

The Oslofjord is somewhat special among the Norwegian fjords from a physical as well as a societal perspective. The population surrounding it, or more precisely people living less than one hours drive from the Oslofjord, comprises 40% of the Norwegian population according to the official statistics⁴. This is by far the most populated area in Norway, a population that is steadily growing. Moreover, no other fjord has anything close to as high density of leisure boats. In addition the Oslofjord features two of Norway's national

⁴<http://www.ssb.no> as of July 1, 2012



Figure 4: Map (left) showing the location where the ship “Godafoss” (right) grounded February 17, 2011. The location is in the sound Løperen between two of the major islands in the Hvaler Archipelago where Norway’s largest river flows through on its way to the Oslofjord.

underwater parks, the Hvaler National Park⁵ and the Færder National Park⁶. Thus, taking into account that the Oslofjord has the largest traffic density of commercial vessels of all the Norwegian fjords the risk of an accident resulting in a possible, unwanted contaminated effluent to the fjord is uncomfortably high⁷.

An example of such an unwanted event is the Godafoss accident. On February 17, 2011 the ship “Godafoss” grounded in a narrow sound in the Hvaler Archipelago (Figure 4), and a lot of its fuel oil leaked into the fjord. As part of the governmental emergency preparedness MET Norway’s task is to forecast the dispersion, drift and spreading of the oil no later than half an hour after the accident⁸. As a matter of fact most of the accidents like Godafoss tend to happen close to the coast or within archipelagos⁹. The safety of the people that utilize the fjord, and the protection of its environment, is therefore a challenge to governmental agencies, regional administrations and local management alike.

Together with wind and waves, ocean currents, temperature and salinity are key in-

⁵<http://www.ytrehvaler.no/>

⁶<http://prosjekt.fylkesmannen.no/faerdernasjonalpark/0m-Farder-nasjonalpark/>

⁷According to DNV report: <http://www.kystverket.no/contentassets/0f030086ed6e4b1aa9f00ac1cd027016/sannsynlighet-for-akutt.pdf>

⁸On behalf of the Norwegian Coastal Administration (Kystverket)

⁹https://en.wikipedia.org/wiki/List_of_oil_spills

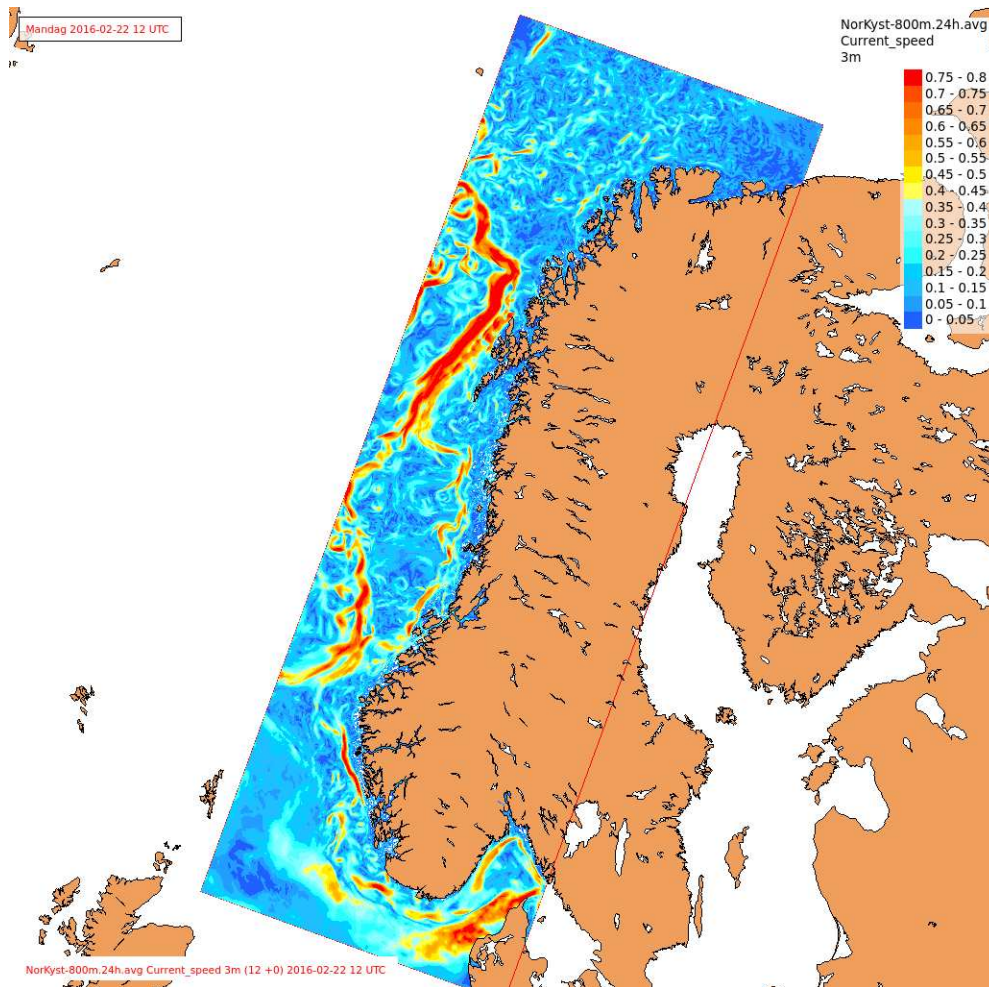


Figure 5: The area covered by the NorKyst800 model. Shown is forecasted, 24 hour average speed at 3 m depth valid for February 22, 2016. Color bar gives speed in m/s with a contour interval of 0.05 m/s.

puts to the model used to forecast oil drift. The present forecasting model providing the latter for the Oslofjord, and run operationally by MET Norway, is the NorKyst800 model (Albretsen *et al.*, 2011). As depicted by Figure 5 it covers the entire Norwegian coast and not only the Oslofjord. In fact it was not developed to capture details within the Norwegian fjords, but rather to capture mesoscale phenomena such as jet currents, eddies and meanders along the the Norwegian coast outside of the fjords. It was set-up with a regular grid of 800x800 m, a grid of high enough resolution to resolve the Rossby radius of deformation required to capture the mesoscale phenomena in Norway’s near coastal waters. Nevertheless, due to its relatively high resolution of 800 m, it was still able to provide forecasts showing some skill even within the fjords.

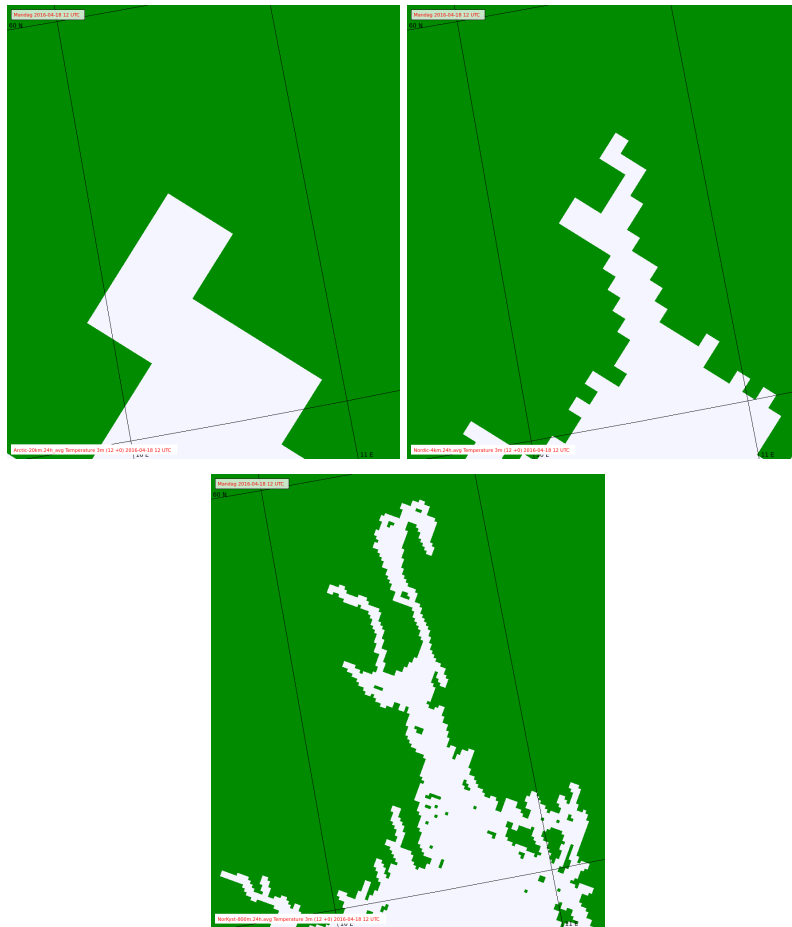


Figure 6: Illustrated is the impact of grid resolution on how the Oslofjord is portrayed. Upper two panels show what the fjord looks like utilizing respectively a 20 km grid (left) and 4 km grid (right). Bottom panel show the same for utilizing a 800 m grid to represent the fjord. As revealed the smaller the grid size (higher grid resolution) the better the coastline geometry is represented.

Despite NorKyst800's relatively high resolution it is still not fine enough to resolve the highly irregular geometry and topography of most Norwegian fjords, and the Oslofjord is no exception. These irregularities consist of small islands, narrow sounds, straits and channels and many smaller scale deep basins and shallow sills as alluded to in Section 1.1 (Figure 1). To properly forecast oil drift, or dispersion of any unwanted substances or contaminants accidentally discharged to the fjord, it is therefore of utmost importance that the underlying fjord model has a realistic representation of the majority of these irregularities.

The aim of the project FjordOs is therefore to develop an Oslofjord model to resolve most of these features without requiring excessive computer power. We emphasize that

such a model, if made operational, will benefit all governmental emergency preparedness models, including those operated by MET Norway. In addition to oil drift these are (i) Search And Rescue or SAR models, which involves forecasting of pathways of floating objects, e.g., man overboard, rafts, small crafts and ships, (ii) transport and spreading of dissolved substances such as nutrients and toxic substances (e.g., nuclear waste), and (iii) growth and drift of toxic algae. Finally we emphasize that resolving the fine scale, submesoscale motion due to the fjord's irregular geometry and topography is required to avoid floating objects, dissolved substances and oil from stranding artificially.

A visualization of the impact of resolution on how well the model portrays these irregularities is depicted by Figures 6. As is evident it is only the 100 m grid that represents the Oslofjord as we know it from geographical charts and maps. An example is the small islands in Breidangen (Tofteholmen and Mølen simply not present in the 800 m grid model. Likewise the shape and area covered by Bastøy is improved in the 100 m grid, and so is the ridge that cuts into the the Drammensfjord at Svelvik. The same is true regarding topography. Figure 7 compares the topography of the NorKyst800 model to the actual topography, as represented in a nautical chart.

To conclude; today's forecasting model available for the Oslofjord (NorKyst800) has an insufficient resolution to properly resolve the small physical scales of the Oslofjord, and a new model with a resolution of 100 m or less for most parts of the fjord is needed. The development of a such a model would also greatly benefit all governmental emergency preparedness models including those operated by MET Norway.

1.3 Organization of the report

Notwithstanding that the purpose of this report is to document the technical details regarding the development of the new Oslofjord model FjordOs CL, we have included above some of the characteristics of the Oslofjord (Section 1.2), and provided some of the motivation why a new Oslofjord model is needed (Section 1.1). Section 2 provides some details on how the curvilinear grid of the FjordOs CL model is constructed. Section 3 provides some model specifics while Section 4 gives details on the model's bathymetry and external forcing such as tides, ocean input through open lateral boundaries, river input as well as atmospheric input. Section 5 provides some results from an almost two year long hindcast. Finally we offer a summary and some concluding remarks in Section 6.

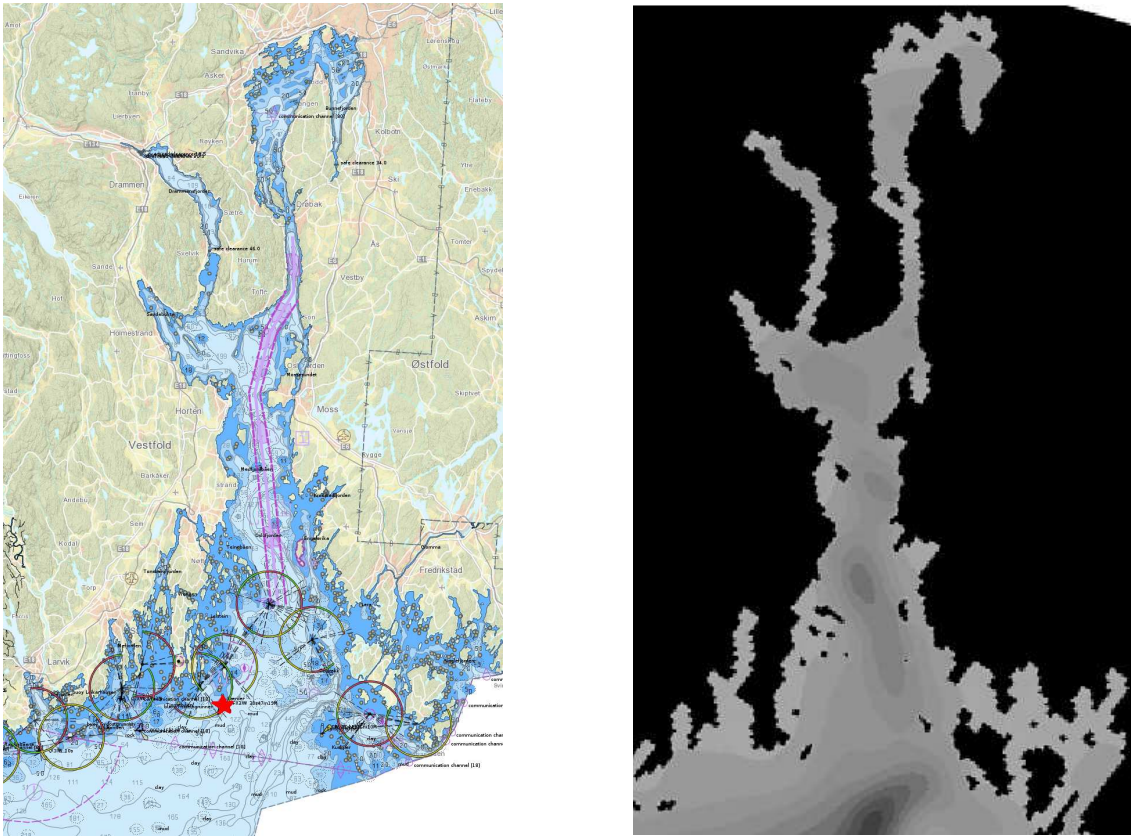


Figure 7: The irregular coastline geometry and topography in the Oslofjord as portrayed in maps (left-hand panel) and the NorKyst800 model (right-hand panel). The red star sign marks the location of the Færder lighthouse. Note the difference in size and depth of the major Hvalerdjupet basin near the southern boundary and the general smoothness of the NorKyst800 topography compared to the real topography.

2 The new model

The FjordOs CL model is based on version 3.6 of the Rutgers Regional Ocean Modeling System (ROMS) adapted to the Oslofjord. ROMS is an open source, numerical ocean model as detailed and documented by *Haidvogel et al. (2008)*, *Shchepetkin and McWilliams (2003)* and *Shchepetkin and McWilliams (2005, 2009)*. It is freely available and may be downloaded from the ROMS website¹⁰.

In summary ROMS is a free-surface and terrain-following, vertical coordinate ocean model, based on the fully three-dimensional, rotational RANS¹¹ equations utilizing the

¹⁰<http://www.myroms.org/>

¹¹Reynolds Average Navier-Stokes

hydrostatic and Boussinesq approximations. It is a so called split–explicit model where short time steps are used to advance the surface elevation and barotropic momentum equation, and where a much larger time step is used for temperature, salinity, and baroclinic momentum. In this ROMS employs a two-way time-averaging procedure for the barotropic mode which satisfies the 3D continuity equation.

2.1 Why ROMS?

An option in ROMS is to use a curvilinear, near orthogonal grid to replace the default orthogonal regular mesh. This option is exploited here. The rationale is that it allows us to minimize the number of, or in reality the area of, “dry” grid points. Thereby the number of “wet” grid points is maximized without increasing the number of grid points compared to an orthogonal, regular grid mesh model covering the same domain. Thus resolution is increased without increasing the computational burden. In addition it allows us, to a certain extent, to put higher resolution in areas of special interest.

The above may also be achieved using unstructured grid models (e.g., FVCOM¹², SLIM¹³). However, the FjordOs research group opted to go for a ROMS development utilizing its curvilinear option rather than starting a completely new strand of model development. The rationale is that 1) ROMS is MET Norway’s operational model, 2) MET Norway’s scientists are well versed in using ROMS, and 3) MET Norway’s scientists have the necessary expertise to operate it. Moreover, none of researchers within the FjordOs participating institutions have any beforehand experience in running and/or setting up a three-dimensional, unstructured model. Nevertheless, to get some insight into the capabilities of an unstructured model, a *two-dimensional version* of FVCOM was used as part of the FjordOs project for the work regarding Moss Harbor (*Hjelmervik et al.*, 2014).

2.2 The curvilinear FjordOs CL grid

Our implementation is inspired in parts by models like the ChesROMS¹⁴ model that applied the curvilinear option for an implementation of ROMS for Chesapeake Bay. There exists several different software packages (MATLAB, Fortran, Python, etc.) that can be used for creating curvilinear grids with variable horizontal resolution for ROMS. We use

¹²<http://fvcom.smast.umassd.edu/fvcom/>

¹³<http://sites.uclouvain.be/slim/>

¹⁴<http://ches.communitymodeling.org/models/ChesROMS/>

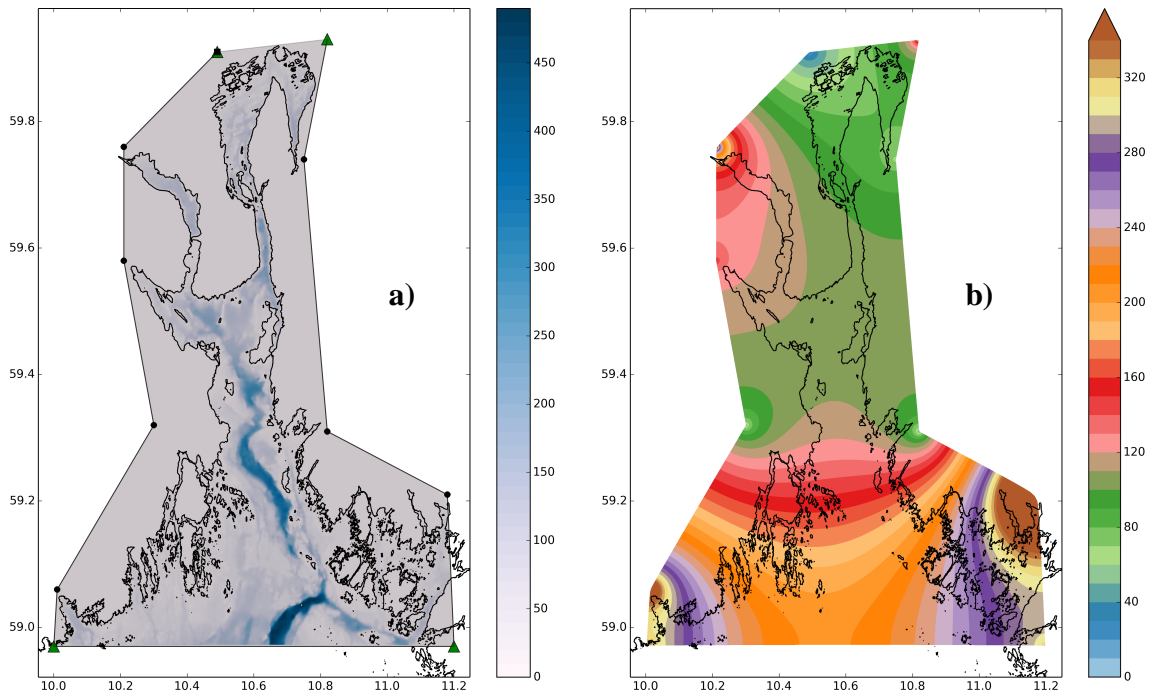


Figure 8: The FjordOs CL computational domain showing (a) the curvilinear grid configuration, and (b) the resulting grid resolution. The right-hand color bar indicates grid size in meters, while the left-hand bluescaled colorbar indicates depth in meters. X-axis is degrees east, and y-axis is degrees north.

the python-based software package OCTANT¹⁵. The outer borders of the model domain is defined by corners and nodes as depicted in Figure 8 where corners are depicted as triangles and the nodes as circular dots. There should be a total of exactly four corners to limit the domain. “Bends” or nodes in the side walls are then specified so as to follow the land-sea matrix. For this first version of the FjordOs model, we have chosen the corners and nodes using a “trial-and-error” approach, so the geometry might be changed in future versions of the FjordOs CL model.

When creating the grid the main constraint is that the grid should be as close to being orthogonal as possible in particular at wet points. One of the advantages of using a package, as for instant the OCTANT package, is that it automatically achieves an optimal orthogonality. To help OCTANT achieving this we have kept the corners and nodes at dry points. The resulting model grid consists of 300 x 900 grid points in the horizontal. As

¹⁵<https://github.com/hetland/octant>

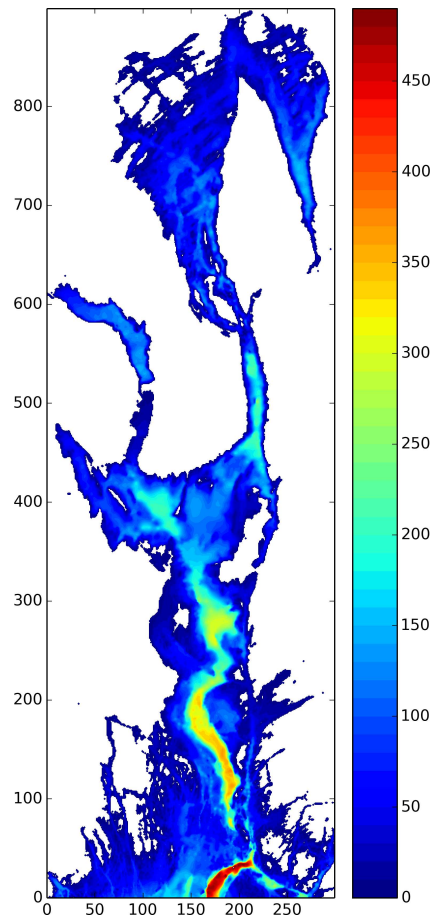


Figure 9: The transformed curvilinear grid of the Oslofjord. The colors gives the depth in meters according to the color bar to the right. Model grid numbers associated with the curvilinear grid are given along the axes. There are 300 x 900 grid points.

shown by Figure 8 the grid size is less than 200 m in most of the wet areas of the fjord, and less than 100 m in most areas north of Slagentangen (at 59.3N). The exceptions are locations along and close to the southern border where the fjord widens and borders on Skagerrak. Here the grid size of the wet points varies from 200 to 350 m. The increased resolution is perhaps best visualized by Figure 9 displaying the Oslofjord in the curvilinear grid coordinates. Recall that in this coordinate system the grid points are equally spaced. Thus Breidangen and the inner Oslofjord is stretched out in the east-west direction. In reality Breidangen is about one third of the geographical distance across the southern open boundary. Thus the resolution in Breidangen and the inner Oslofjord is in effect increased with a factor of three. In the Drøbak sound the east-west grid size in the curvilinear grid is about 80 m.

3 Model specifics

The version of ROMS we use is downloaded from the main ROMS repository¹⁶, and includes the 3.6 version of the code from Hernan Arango (the Rutgers branch). This version is without sea ice, but in contrast to most other ROMS versions allows data assimilation.

ROMS consists of several built-in schemes and algorithms, and it uses C-preprocessing to activate the various physical and numerical options. ROMS is a very up-to-date and modular code written in F90/F95. The entire input and output data structure of the model is via NetCDF which facilitates the interchange of data between computers, user community, and other independent analysis software.

In the horizontal the model state variables are staggered using an Arakawa C-grid as shown by Figure 10. The free-surface, density, and active/passive tracers are located at the center of the cell (ρ points) whereas the horizontal current components (u , v) are located at the west/east and south/north edges of the cell, respectively. In ROMS all the arrays containing state variables are dimensioned with the same size in the horizontal to facilitate parallelization. The size of the model's horizontal grid is defined in the ROMS input file (`ocean.in`) with interior points only (denoted $L - 1$ and $M - 1$ in Figure 10). However, all input forcing files must, and output result files do, contain fields at the full grid, which includes the one extra grid point in the boundary zone.

In the vertical ROMS make use of a stretched terrain-following coordinate denoted $s = s(x, y, z, t)$, sometimes referred to as modified σ -coordinates (Song and Haidvogel, 1994). As a result, each grid cell has a different level thickness (denoted $H_z = \partial_s z$) and volume. The model state variables are vertically staggered so that horizontal momentum, density, and active/passive tracers are located at the center of the grid cell. The vertical velocity and vertical mixing variables (Akt , Akv , etc) are located at the bottom and top faces of the cell as displayed by Figure 11. The stretched coordinate allows increased resolution in areas of interest, such as thermocline and bottom boundary layers.

Regarding the FjordOs CL model we opted for 42 s -layers with an increased resolution in the surface layer and a reduced resolution near the bottom. This was achieved by letting $Vtransform = 2$, $Vstretching = 4$, $h_c = 50$ m, $\theta_s = 3.0$ and $\theta_b = 0.5$, where h_c is a critical depth above which the vertical spacing of the s -levels become nearly uniform and independent of the local depth h as long as $h \gg h_c$. The minimum depth was set to

¹⁶<http://www.myroms.org/svn/src/tags/roms-3.6/>

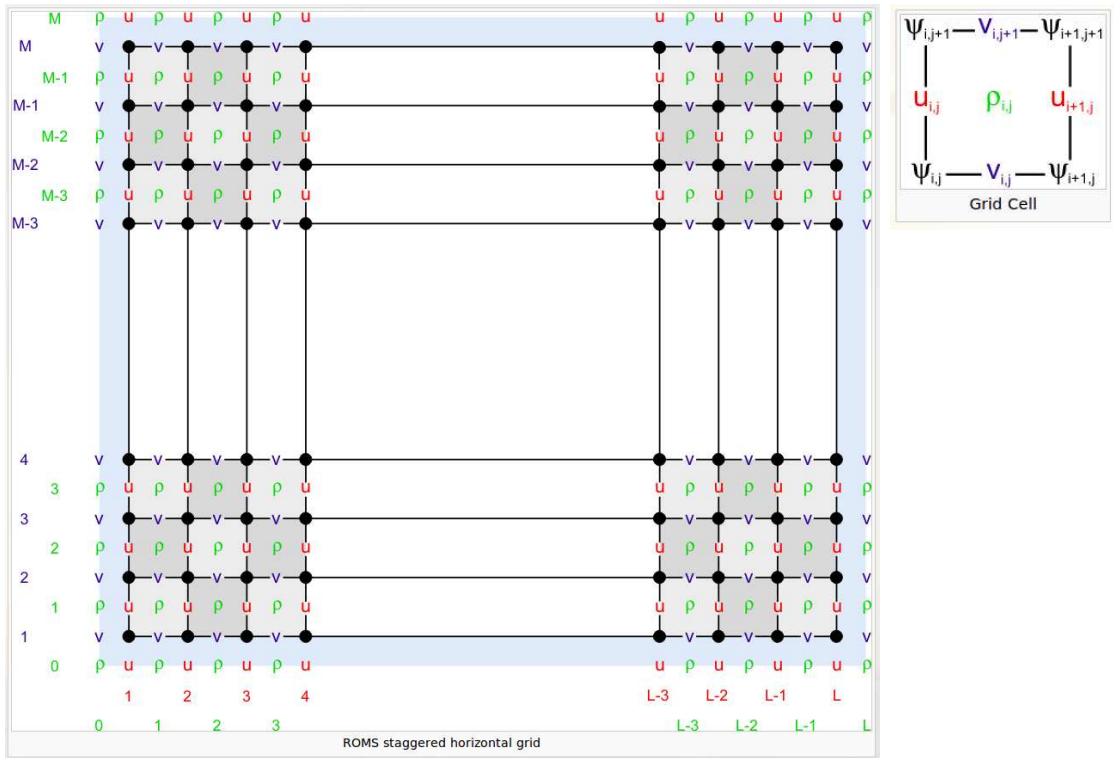


Figure 10: The horizontal distribution and numbering system of variables in the ROMS grid. The figure is downloaded from the <http://www.myroms.org> website.

$h_{min} = 2$ m. By having the s -levels more confined to the surface layers less smoothing is necessary to minimize the pressure gradient error inherent in all terrain-following coordinate models (Haney, 1991). The smoothing is controlled by two parameters referred to as the r -factors (see Section 4.1). An example of the vertical distribution of the s -levels is shown by Figure 12.

ROMS has several options that determines the numerical schemes for lateral advection of momentum and tracers. In the results displayed in Section 5, we have employed a fourth-order, centered advection scheme. This necessitate the application of explicit lateral eddy viscosity and diffusion. To parametrize the subgrid-scale vertical mixing processes we use the Generic Length Scale (GLS) scheme (Umlauf and Burchard, 2003). Values chosen for the various parameters and options activated to derive the results exhibited by Section 5 are listed in Table 1.

To run the model several external inputs or forcing have to be supplied, such as atmospheric input, river input, tides, and input of sea level, currents and hydrography at the model's open lateral boundaries, in addition to bathymetry as described in Section 4.

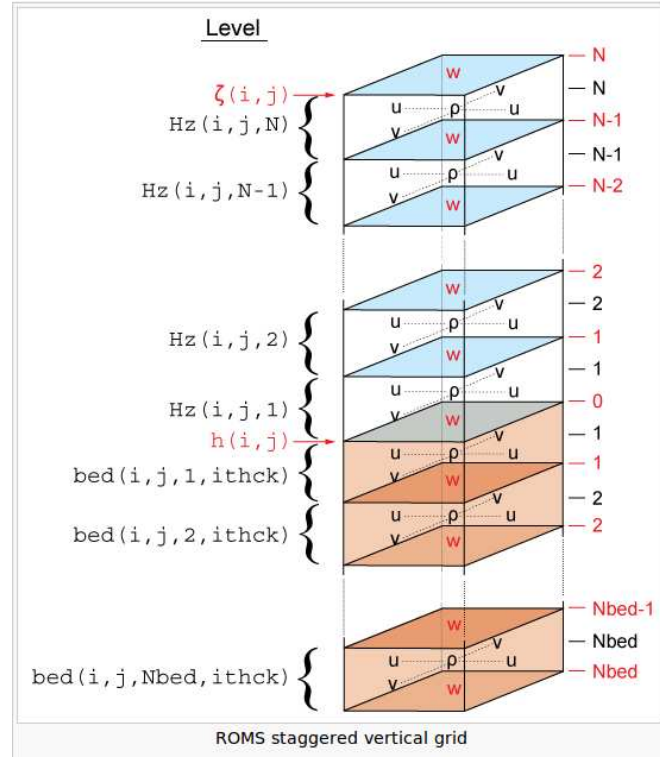


Figure 11: The vertical distribution and numbering system of variables in the ROMS grid. The figure is downloaded from the <http://www.myroms.org> website.

4 Bathymetry and external forcing

4.1 Bathymetry

The bathymetry data for the FjordOs CL model is supplied by NIVA. The original resolution was 25 m. Modifications of some of the topographical features were needed to fulfill the restriction of avoiding one-point bays in ROMS. Additionally, effort was made in opening up narrow straits important for the local circulation, in particular advection of brackish water originating from rivers. To avoid model instability and/or spurious deep currents the final masked bathymetry is smoothed to fulfill a requirement on the ROMS slope or r_{x0} -factor (*Beckmann and Haidvogel, 1993*), defined as

$$r_{x0} = \frac{h_{i-1} - h_i}{h_{i-1} + h_i} \quad (1)$$

where h is the bottom depth and the index i indicates a model grid point. The final bathymetry in FjordOs CL has a maximum $r_{x0} = 2.372424E - 01$.

In addition, Haney (1991) argues that in order for difference schemes to be hydrostat-

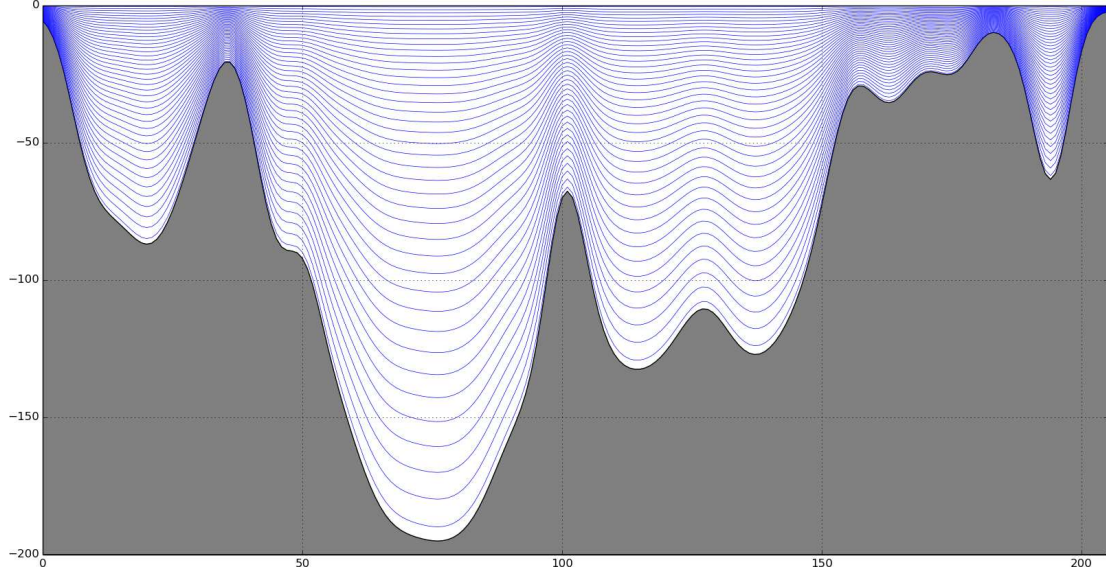


Figure 12: Sketch of the vertical distribution of s -levels in the FjordOs CL model (cross-section at Breidangen, $y=600$).

Table 1: List of FjordOs CL model set-up parameters.

Parameter	Symbol	Value	Unit
Vtransform	-	2	-
Vstretching	-	4	-
Number of layers	k	42	
Critical depth	h_c	50	m
Surface resolution factor	θ_s	3.0	-
Bottom resolution factor	θ_b	0.5	-

ically consistent, the parameter settings must be defined so that

$$\left| \frac{s}{h} \partial_x h \right| \frac{\Delta x}{\Delta s} < 1 \quad (2)$$

where s denotes the value of the terrain-following s -layer (0 at the surface, -1 at the bottom), $\partial_x h$ is the difference in depth over a grid cell, Δx is the grid size and Δs is the vertical distance between s -layers. For instance in a grid cell with total depth of $h_i = 1000$ m, with a neighboring depth of $h_i - 1 = 900$ m, with a grid resolution $\Delta x = 800$ m, near the seabed between s -layer 0.9 and 1.0, the Haney number would be 1. In practice the Haney number is estimated by

$$r_{x1} = r_{x0} \frac{Z_w(i, j, k) - Z_w(i-1, j, k) + Z_w(i, j, k-1) - Z_w(i-1, j, k-1)}{Z_w(i, j, k) + Z_w(i-1, j, k) - Z_w(i, j, k-1) + Z_w(i-1, j, k-1)} \quad (3)$$

where Z_w is the depth of the water column at grid coordinates (i, j) and at s level k . In the case where the second deepest s -level of grid cell (i, j) has equal depth to the deepest level in grid cell $(i - 1, j)$ the Haney number will be 1. Obeying the criteria (2) ensures that for a certain grid size the vertical grid increment is small enough for the s -layer immediately above (below) remains above (below) within the distance of one grid interval. Although there is no mathematically well-defined thresholds a rule of thumb is $r_{x1} \lesssim 10$. There is no consensus in the ROMS community on the upper limit for r_{x1} though. Thus one has to consider the recommendations on thresholds to be the outcome of practical experience. For instance Kate Hedstrøm allows a Haney number of several tens while Alexander Shchepetkin considers a value below 3 as “safe and conservative” and values above 8-10 as “insane”¹⁷. It boils down to controlling the pressure gradient error. FjordOs CL has a maximum $r_{x1} = 1.424997E + 01$.

4.2 Atmospheric forcing

The necessary atmospheric input is extracted from the AROME-MetCoOp model that runs operationally at MET Norway (*Müller et al., 2015*). It is a convective scale (non-hydrostatic) model providing forecasts with a lead time of 66 hours four times a day from analyses at 00, 06, 12 and 18 UTC. It has a grid resolution of 2.5 km, and was made operational in March 2014. Available to us are analyses and forecasts saved every six hours since April 2014, as well as real time forecasts covering the are shown in Figure 13.

We extract from AROME-MetCoOp, as listed in Table 2, surface analysis and forecasts of wind, pressure, temperature, humidity and cloud cover daily at 00, 06, 12, 18 UTC. Rainfall rates was calculated by using the accumulated rainfall at +6 hours lead time. AROME-MetCoOp store all these parameters at its grid resolution. From these parameters and variables fluxes are computed using the internal bulk-flux routines in ROMS (e.g., *Røed and Debernard, 2004*). FjordOs CL also computes internally, from analytic expressions, net long wave radiation and short wave radiation.

4.3 Input at open lateral boundaries

4.3.1 De-tided input

¹⁷ROMS Discussion Forum (<https://www.myroms.org/forum/viewtopic.php?f=14&t=612>)

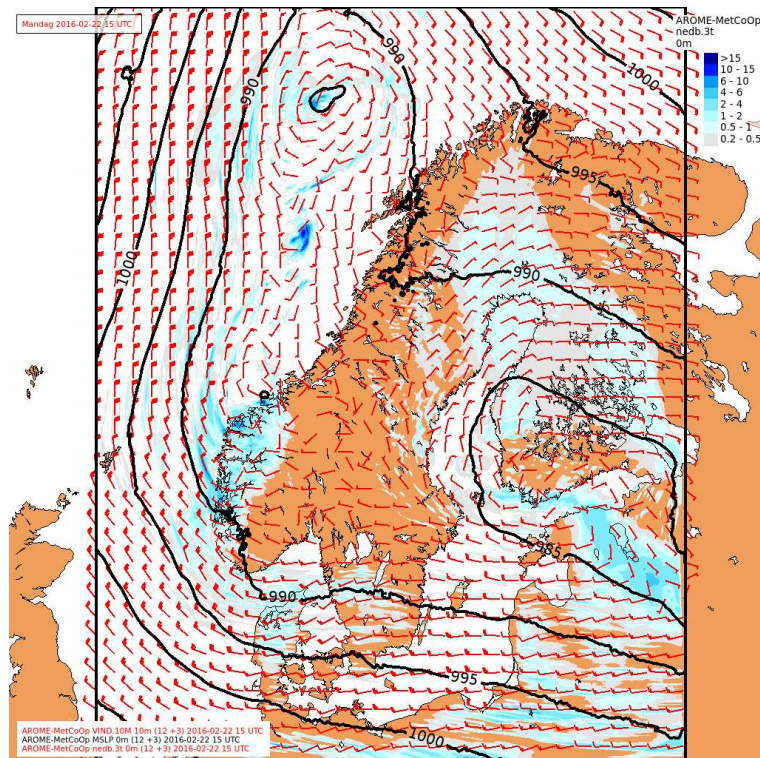


Figure 13: The area covered by the Arome-MetCoop model. Shown is the forecasted (lead time 3 hrs) mean sea level pressure in hPa (black solid lines, countour interval = 5 hPa), 3 hourly precipitation, and 10 m wind valid at 1500UTC on February 22, 2016. Color bar indicates precipitation with a variable contour interval in the range 0.2-15 mm or larger (deep blue).

The FjordOs CL grid has one wide open boundary located at its southern end towards the Skagerrak. Here we use input from the NorKyst800 model in the form of daily mean (dedided) values of sea level, currents and hydrography. The NorKyst800 model covers the Norwegian coast including the Skagerrak and the Oslofjord with a grid resolution of 800 m as shown by Figure 5. To include the forcing from the NorKyst800 model a one-way nesting technique is employed as described in *Marchesiello et al.* (2001).

The NorKyst800 is run operationally at MET Norway once a day and provides hourly forecasts with a lead time of 66 hrs. Daily mean values are computed and stored as netCDF files. These fields with some modifications may in addition be used as initial values to "semi-hot" start FjordOs (Section 5). The archive containing daily mean values is updated automatically and adds back to 2012. The hourly forecast values are stored and archived one week back in time only. Both archives are available from MET Nor-

Table 2: List of atmospheric forcing parameters.

Parameter name	ROMS	
	input name	Unit
10 m U wind component	Uwind	ms^{-1}
10 m V wind component	Vwind	ms^{-1}
2 m air temperature	T_{air}	$^{\circ}\text{C}$
Mean sea level pressure	P_{air}	hPa
Total cloud cover	cloud	fraction
Specific humidity	Q_{air}	g kg^{-1}
Total precipitation	rain	$\text{kgm}^{-2}\text{s}^{-1}$

way's thredds server¹⁸. As input at the lateral open boundary FjordOs CL requires daily mean sea level values in addition to daily mean depth profiles of currents temperature and salinity.

4.3.2 Tidal forcing

The daily mean values extracted from NorKyst800 are viewed as being crudely de-tided. To get tides into the FjordOs CL model, tidal elevation and tidal (barotropic) currents have to be specified separately and superimposed on the daily mean NorKyst800 input.

The tidal input in terms of tidal elevations and currents are based on the TPXO Atlantic database (*Egbert and Erofeeva, 2002*, hereafter ATPXO)¹⁹. Before supplying them to the FjordOs CL model they were first modified using measured tides at the Viker tidal gauge station located close to the southern boundary in the Hvaler Archipelago. Included are the nine tidal constituents listed in Tables 3 and 4. As is evident semi-diurnal constituent M_2 is by far the most dominant one, but also N_2 and S_2 contributes.

The rationale for the modification of the tidal input is that the resolution of the ATPXO, which is $1/30^{\circ}$, is too coarse to get the exact phase and amplitude of the tides in Skagerrak correct. To modify the tides we first imposed the nine constituents on the open boundary of tides from the ATPXO database, and let it run for more than a year (the actual period was 12:00 UTC, April 1, 2014 - 12:00 UTC, September 28, 2014). Time series of water level from a location near the Viker and Oscarsborg tidal gauge stations were

¹⁸<http://thredds.met.no/thredds/fou-hi/norkyst800m.html>

¹⁹<http://volkov.oce.orst.edu/tides/A0.html>

Table 3: Simulated tidal amplitudes [cm] and phases [deg] for a location close to the Viker tidal gauge station. The column "ATPXO" refers to the simulated tides using the TPXO Atlantic data base as input, while the column "Modified" refers to a run using adjusted tides as input. The column "Observed" refers to the observed tides at the nearby Viker tidal gauge station and is added for comparison.

Constit.	Period [hrs]	Observed		ATPXO		Modified	
		[cm]	[deg]	[cm]	[deg]	[cm]	[deg]
M ₂	12.4206	12.4±0.7	115±3	9.7±1.1	122±6	11.8±0.3	105±1
N ₂	12.6583	2.8±0.7	69±14	5.7±1.1	81±11	3.1±0.3	69±5
S ₂	12.0000	2.3±0.7	48±15	5.1±1.0	81±11	3.2±0.3	67±5
O ₁	25.8193	2.1±0.7	282±20	3.7±0.4	19±8	2.9±0.2	338±3
M ₄	6.2103	1.4±0.2	287±7	0.7±0.2	25±17	1.1±0.0	354±1
Q ₁	26.8684	1.0±0.6	221±42	0.1±0.3	215±154	0.1±0.1	253±156
K ₁	23.9345	0.7±0.6	98±49	1.2±0.5	212±23	0.1±0.1	198±97
MN ₄	6.2692	0.4±0.2	270±24	1.0±0.2	141±12	0.3±0.0	7±3
MS ₄	6.1033	0.4±0.2	5±28	1.1±0.2	111±12	0.6±0.0	80±1

then extracted and analyzed based on the T_Tide package described by *Pawlowicz et al.* (2002). The results are shown under column "ATPXO" in Tables 3 and 4. For comparison we have also extracted and analyzed the observed time series from the Viker and Oscarsborg tidal gauge stations compiled from the Norwegian Coastal Administration (Tidevannstabeller for den norske kyst med Svalbard, 2008). The result of this analysis is shown in column "Observed", and clearly show that the simulated tides off the mark.

To better match the observations tidal amplitudes and corresponding phases at the Viker tidal gauge station were then modified by computing an amplitude factor, $c^{(n)}$, and a phaseshift, $\Delta\phi^{(n)}$ for each tidal component n according to:

$$c^{(n)} = a_{obs}^{(n)} / a_{sim}^{(n)} \quad (4)$$

$$\Delta\phi^{(n)} = \phi_{obs}^{(n)} - \phi_{sim}^{(n)} \quad (5)$$

where $a^{(n)}$ is the amplitude and $\phi^{(n)}$ is the phase for tidal component number n of the water level in the column "ATPXO". New amplitudes and phases at the boundary were then calculated using the computed amplification factor and phaseshift on both water level and velocity. The modified tides were then supplied to the FjordOs CL and run for a year with tidal forcing only. The new results were then analyzed exactly as for the ATPXO run.

Table 4: As Table 3, but for the Oscarsborg tidal gauge station.

Con-stit.	Period [hrs]	Observed		ATPXO		Modified	
		[cm]	[deg]	[cm]	[deg]	[cm]	[deg]
M ₂	12.4206	14.1±0.7	132±3	11.1±1.2	128±7	13.7±0.3	111±2
N ₂	12.6583	3.0±0.8	85±15	6.6±1.4	86±10	3.6±0.4	75±6
S ₂	12.0000	2.7±0.8	70±18	6.1±1.3	85±11	3.7±0.4	70±7
O ₁	25.8193	2.1±0.7	286±17	3.9±0.5	21±8	3.1±0.2	340±4
M ₄	6.2103	2.1±0.3	332±8	1.4±0.4	44±19	2.0±0.0	14±1
Q ₁	26.8684	1.0±0.7	230±36	0.2±0.4	204±126	0.0±0.2	190±165
K ₁	23.9345	1.2±0.5	101±35	1.1±0.5	213±27	0.1±0.2	44±79
MN ₄	6.2692	0.6±0.3	316±26	2.0±0.4	163±14	0.5±0.0	29±3
MS ₄	6.1033	0.5±0.3	57±32	2.2±0.4	135±11	1.3±0.0	106±1

The resulting new tidal amplitudes and periods for the locations close to the Viker and Oscarsborg tidal gauge stations are shown in Tables 3 and 4 in column “Modified”. The results are clearly improved at both stations. In particular we are pleased with the results close to the Oscarsborg tidal gauge station which may be viewed as a control station in that it is far away from the southern boundary where the tidal forcing is imposed.

4.4 River input

The influence of the freshwater discharged to the Oslofjord by way of the many rivers surrounding it is well known. A relevant example is shown by Figure 20 constructed from a test run with an earlier version of the FjordOs CL model. In particular the impact on the daily mean sea surface salinity of Norway’s two largest rivers, namely Glomma to the southeast and Drammenselva to the northwest, is evident. As shown it tends to create salinity fronts that in turn give rise to high lateral as well as vertical shear currents. From time to time these fronts are even strong enough to generate instabilities. To obtain a realistic, high resolution picture of the circulation in the Oslofjord it is therefore paramount to include the input from these and other smaller rivers.

To obtain the necessary information on the freshwater discharges to the Oslofjord within the FjordOs CL model domain we make use of discharge data from a database constructed by use of the hydrological model HBV (*Beldring et al., 2003*). In essence the HBV model provides an estimate of the daily mean freshwater drained into the ocean (or

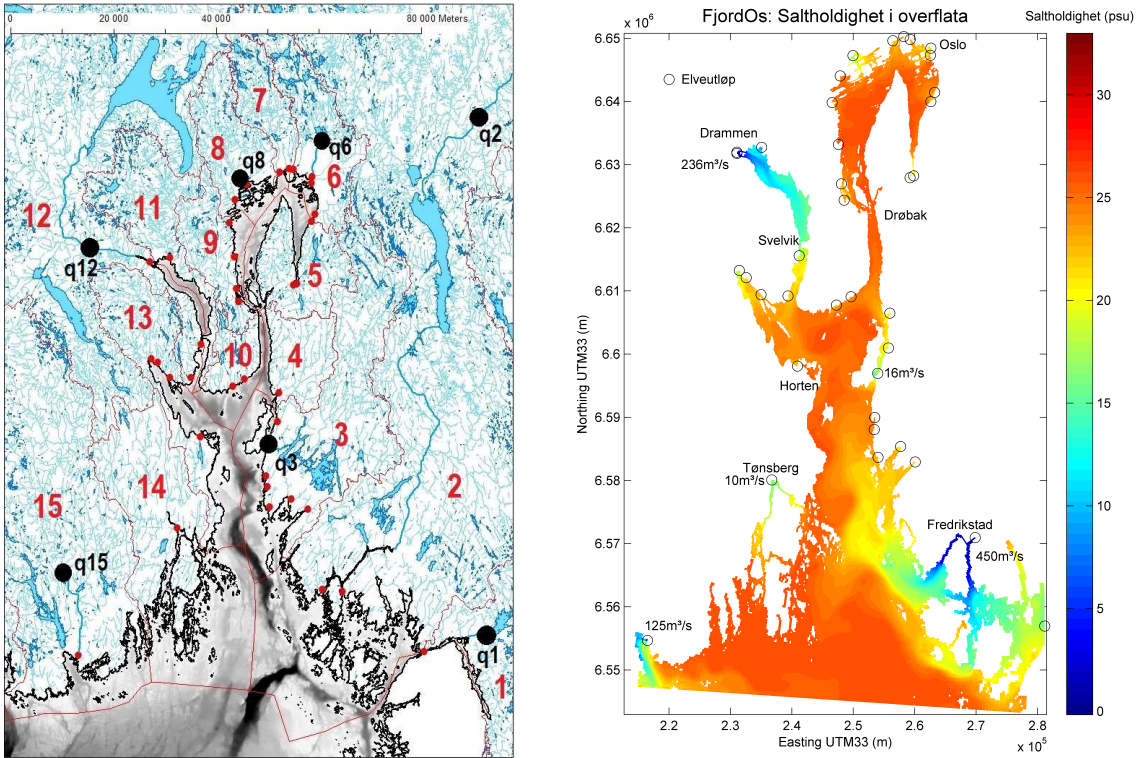


Figure 14: Left panel shows the many rivers (blue solid lines) emptying freshwater to the fjord (from NVE elvenett). The red numbers indicate a Main Catchment Area (MCA). The red dots indicate the location of the individual rivers discharging freshwater to Oslofjord (cf. Table 5). Some of the larger rivers, for instance Glomma, Drammenselva and Numedalslågen, are marked with a thicker blue line. Stations with water discharge measurements are shown with green dots and numbered with black numbers, e.g. q8. Right panel shows the location of the 37 rivers named in Table 5.

fjord) from a preselected set of so called Main Catchment Areas (MCAs). Each MCA has in turn at least one or more rivers with an outlet to the sea. Let Q_i be the daily mean freshwater discharged from the i th MCA and A_i its area. Furthermore, let q_{ij} be the discharge from the j th individual river associated with the i th MCA. Then assuming that q_{ij} is entirely determined by the ratio of its local catchment area a_{ij} to the area of the MCA, that is A_i we get

$$q_{ij} = \frac{a_{ij}}{A_i} Q_i. \quad (6)$$

A total of 15 of Norway's MCAs drains into the Oslofjord within the FjordOs model domain (Figure 14). These MCAs in turn contain a total of 46 river outlets as listed by

Table 5. Six of these belongs to Glomma and five to Drammenselva. Hence there are 37 named rivers. Their locations are shown by Figure 14. By use of (6) and Table 5 we may find the discharge emitted from each of them provided Q_i is known. The HBV database contains information on Q_i from 1962 up to and including the previous year with a lag of about six months. Thus Q_i was not available for 2015 at the time of the simulations presented in this report. Our hindcast period is from April 1, 2014 up to and including December 2015. We must therefore obtain information on Q_i for 2015 from another source. To this end we make use of observations from the NVE website²⁰ available in near real time. If we for instance consider the observed discharge from river n within the i th MCA, we find Q_i by rearranging (6), that is,

$$Q_i = A_i \frac{q_{in}}{a_{in}}. \quad (7)$$

where q_{in} is the known discharge of the n 'th river and a_{in} is the size of its local catchment area. Having thus found Q_i we find the discharges from the remaining rivers of that MCA by use of (6) and the a_{ij} 's listed in Table 5.

Using this method we first calculated the daily mean discharge for MCA numbers $i = 1, 2, 3, 6, 8, 12,$ and 15 using the NVE station data for rivers nos. 1 (Iddefjorden/Haldenv.), 2-7 (Glomma), 13 (Mosseelva), 21 (Akerselva), no. 25 (Sandvikselva), 34-38 (Drammenselva) and 46 (Numedalslågen). The NVE station for MCA no. 2 is located far upriver (Figure 14), so a correction factor is estimated based on a least square fit between the NVE observations at Rånåsfoss and the Glommens og Laagens Brukseierforening (glb.no) observations at Sarpfoss for the period up to and including October 28, 2015. The result is

$$Q_2 = 1.123 \cdot Q_{\text{Rånåsfoss}}. \quad (8)$$

This yields an estimate of the river discharge in Glomma with an RMS error of about $100 \text{ m}^3/\text{s}$. The corresponding discharges, that is, q_{2j} for $j = 2, 3, \dots, 7$, are found by use of (6) and the size of the corresponding local catchment areas a_{2j} listed in Table 5.

Table 5: Rivers in the FjordOs CL model. The outlet positions follow the index convention in ROMS. The position is at a u -point if the direction is along the x -axis, and at a v -point if the direction is along the y -axis. The index counting in ROMS starts at 0, except for the u -points and v -points, where the count starts at 1. MCA: Main Catchment Area.

²⁰<http://www2.nve.no/h/hd/plotreal/q/index.html>

River No.	MCA no.	Area a_{ij}	Outlet x -pos.	Outlet y -pos.	Direction 0=along x 1=along y	Sign	Name
1	1	2512.00	297	44	0	-1	Iddefjorden/Haldenv.
2	2	7222.43	261	77	1	-1	Glomma (Østerelva)
3	2	7222.43	260	77	1	-1	Glomma (Østerelva)
4	2	7222.43	259	77	1	-1	Glomma (Østerelva)
5	2	7222.43	258	70	1	-1	Glomma (Østerelva)
6	2	7114.64	248	91	0	-1	Glomma (Vesterelva)
7	2	7114.64	248	92	0	-1	Glomma (Vesterelva)
8	3	13.90	273	202	0	-1	Krokstadbekken
9	3	25.90	251	230	1	-1	Heiabekken+Kureåa
10	3	7.57	213	219	1	-1	Støtvikbekken
11	3	3.83	211	258	1	+1	Evjeåa
12	3	5.55	213	275	1	-1	Gunnarbybekken
13	3	688.34	221	337	0	-1	Mossevassdraget
14	3	19.33	239	373	0	-1	Kambobekken
15	4	138.49	242	423	0	-1	Hælenelva
16	5	6.94	273	634	1	+1	Gloslibekken
17	5	51.72	280	638	1	+1	Årungelva
18	5	85.97	286	784	0	-1	Gjersjøelva
19	6	39.10	289	802	0	-1	Ljanselva
20	6	69.26	267	864	0	-1	Alna
21	6	237.81	266	876	1	-1	Akerselva
22	6	23.24	226	890	1	-1	Frognerbekken
23	7	14.46	213	895	0	-1	Hoffelva
24	7	176.30	188	888	1	-1	Lysakerelva
25	8	227.72	83	843	1	-1	Sandvikselva
26	8	21.74	72	782	1	-1	Neselva
27	9	37.63	84	726	1	+1	Askerelva

continued on next page

continued from previous page

River No.	MCA no.	Area a_{ij}	Outlet x-pos.	Outlet y-pos.	Direction 0=along x 1=along y	Sign	Name
28	9	2.82	126	665	1	+1	Nærsneselva
29	9	112.95	149	607	0	+1	Årosvassdraget
30	9	19.05	158	584	0	+1	Sætreelva
31	10	18.01	179	447	1	-1	Tofteelva
32	10	35.47	156	435	1	-1	Sageneelva
33	11	309.38	22	621	1	-1	Lierelva
34	12	2139.31	1	611	0	+1	Drammeneslva 1
35	12	4278.61	1	610	0	+1	Drammenseslva 2
36	12	4278.61	1	609	0	+1	Drammenseslva 3
37	12	4278.61	1	608	0	+1	Drammenseslva 4
38	12	2139.31	1	607	0	+1	Drammeneslva 5
39	12	8.11	97	501	1	-1	Ebbestadelva
40	12	14.54	82	447	0	+1	Bergerelva
41	13	6.59	42	450	1	-1	Sandobekken
42	13	29.84	22	472	1	-1	Selvikelva
43	13	193.23	13	481	1	-1	Sandevassdraget
44	13	33.66	93	351	1	+1	Borreelva
45	14	1115.00	61	186	0	+1	Aulivassdraget
46	15	6514.00	9	23	0	-1	Nummedalslågen

For some of the 15 MCAs in the model domain, no observations are available ($i = 4, 5, 7, 9, 10, 11, 13, 14$). We have estimated Q_i for these rivers using the Q_i 's from MCA nos. 2 (Glomma), 3 (Mosseelva), 8 (Sandvikselva) and 15 (Nummedalslåen). An auxiliary parameter was calculated that was the sum of the river discharges of all combinations of the four rivers. A least mean square fit was performed between this new parameter and the discharge for the MCA in question, namely

$$Q_i = \alpha_i (f_{i2}Q_2 + f_{i3}Q_3 + f_{i8}Q_8 + f_{i15}Q_{15}) + \beta_i. \quad (9)$$

The result of this analysis is shown in Table 6. It is somewhat surprising that the discharge from MCA nos. 2 and 15 did not influence the estimate of the discharge from the other

Table 6: Estimating discharges in unobserved MCAs based on observations at four MCAs with observations using the least mean square fit (9).

MCA	f_{i2}	f_{i3}	f_{i8}	f_{i15}	α_i	β_i
no.						
4	0	1	0	0	0.201	0.120
5	0	1	0	0	0.265	0.274
7	0	0	1	0	0.625	0.531
9	0	0	1	0	0.750	0.209
10	0	0.5	0.5	0	0.264	-0.276
11	0	0	1	0	1.317	0.417
13	0	0	1	0	1.081	0.998
14	0	0.5	0.5	0	1.000	1.087

MCAs.

Finally we emphasize that the rivers, in addition to providing freshwater to the fjord, are sources of nutrients, organic matter, bacteria, particles and contaminants. Several of these parameters are monitored in the national monitoring program (Riverine Inputs and direct Discharges - RID, *Skarbøvik et al.*, 2011). It is therefore possible to include information from the RID program in the river forcing, and hence the FjordOs CL model may be used in the future to model dispersion of any of the RID parameters.

5 Sample results

All the results shown below are derived by running FjordOs CL on the Vilje supercomputer at the Norwegian High Performance Computing facilities in Trondheim. We show results from a hindcast initialized from NorKyst800 on April 1st, 2014 and continued up to and including the month of December 2015. All inputs are as described in Section 4.

The results from the hindcast are further discussed and evaluated in some detail in an upcoming report (*Hjelmervik et al.*, 2016). Here we merely present snapshots of fields of currents, temperature, salinity and sea level at 2 meters depth on March 23, 2015, that is, about one year after commencing the simulation. To properly appreciate the level of details provided by the FjordOs CL model the simulated currents are shown for selected parts of the fjord (Section 5.1). Regarding hydrography and sea level (Section 5.2), the whole computational domain covered by the FjordOs CL model is displayed.

5.1 Currents

We first note the detailed current pattern returned by the FjordOs CL model as shown by Figures 15 - 19. Although the speed in the inner Oslofjord (Figure 15) is low compared to other parts of the fjord, e.g. in the Drøbak Sound (Figure 16) the pattern is nevertheless as rich in detail as in the rest of the fjord.

Current at 2 m depth - 27-03-2015 13:00 UTC

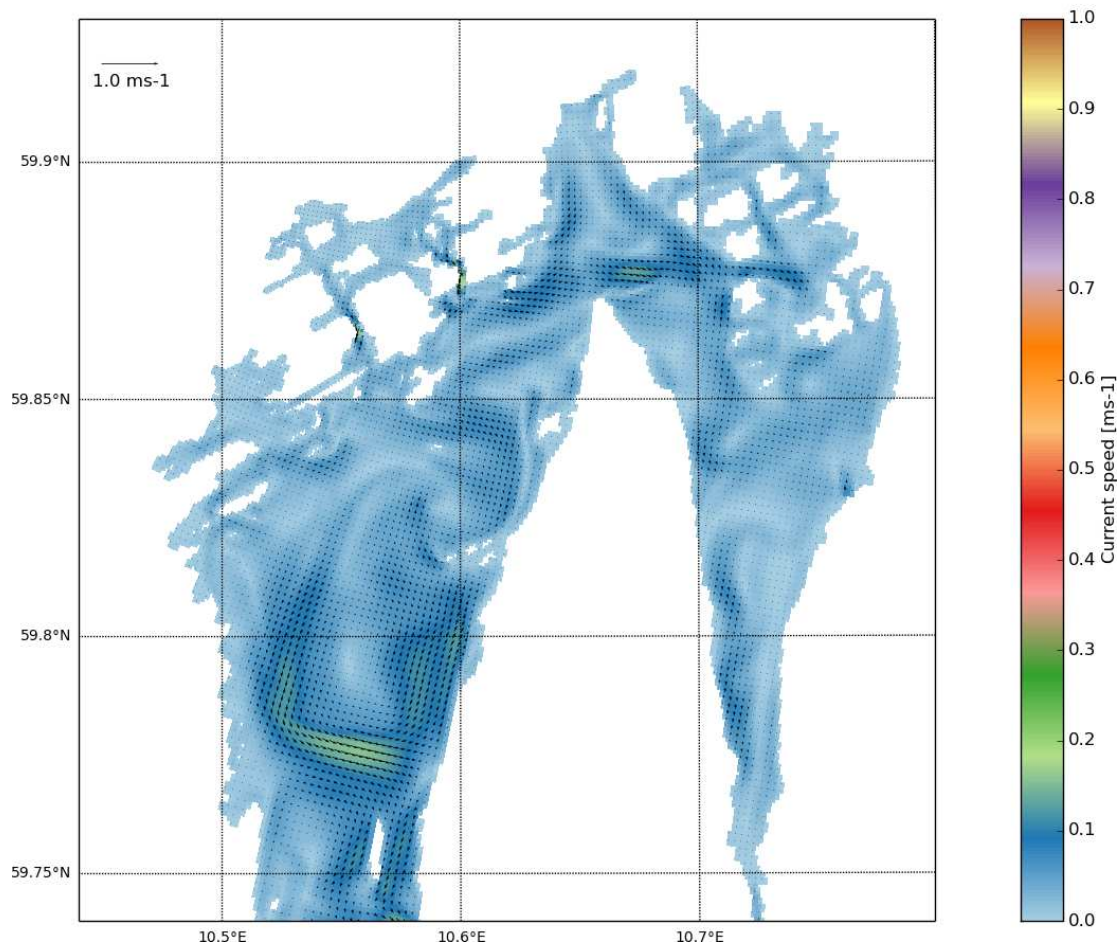


Figure 15: Currents at 2 meter depth for the inner part of the Oslofjord (including Bunnefjorden and Oslo Harbour).

As revealed by Figure 16 the speed in the Drøbak Sound is much stronger with speeds bordering on 1 m/s. We also note the presence of the Jetty obstructing the western southward flow to pass through the two narrow openings in the Jetty. The picture is one of a strong outflow in which the flow in the Drøbak Sound is a jet hugging more or less the

Current at 2 m depth - 27-03-2015 13:00 UTC

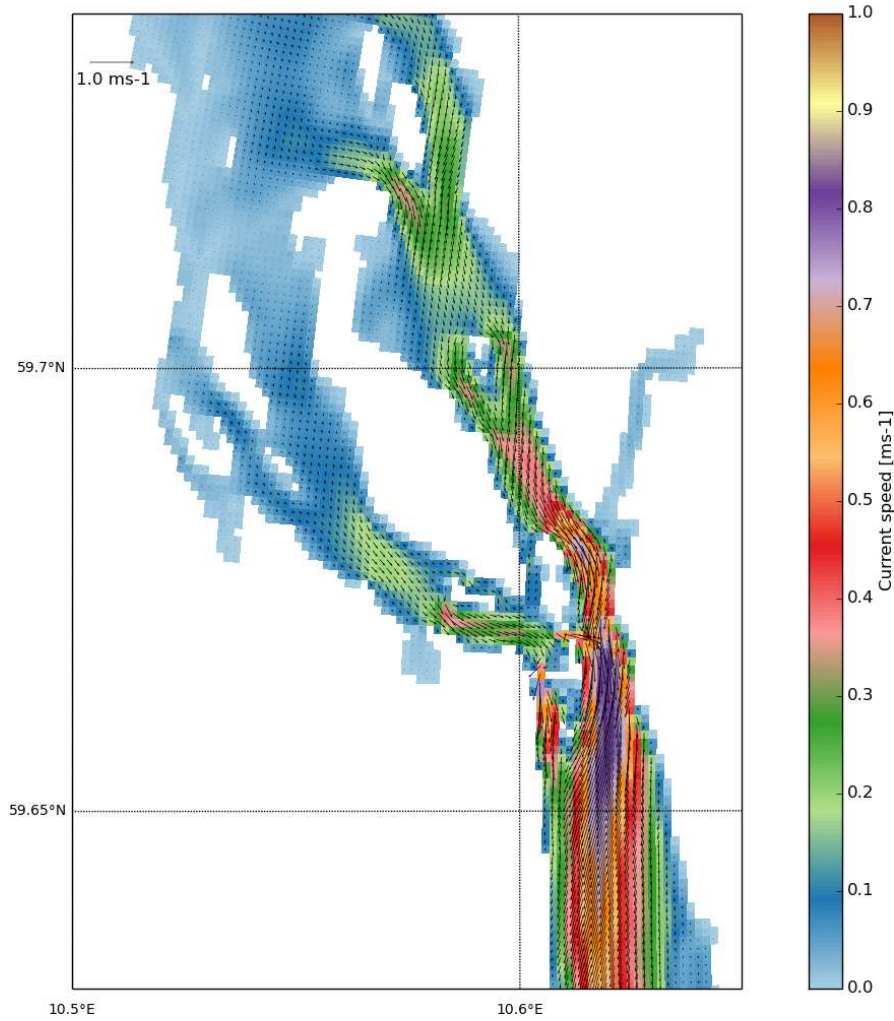


Figure 16: As Figure 15, but for the Drøbak Sound and Vestfjorden area.

western bank due to the effect of the Earth's rotation.

As we proceed southwards into Breiangen the fjord widens (Figure 17). The jet like outflow from the Drøbak Sound continues southward and is clearly guided by the topography. Nevertheless, rich details in the current patterns on its flanks are clearly visible. As revealed also Drammenselva is discharging its water into Breiangen through the Drammensfjord. Note that the simulation replicates the swift current through the narrow opening between Drammensfjorden and Breiangen at Svelvik.

Moving further south the topography usher the jet like outflowing current to follow the deeper parts of the fjord. Hence it meanders southward toward Bolærne (Figure 18). Due to the strong main outflow we observe that water is forced to flow through many of

Current at 2 m depth - 27-03-2015 1

Current at 2 m depth - 27-03-2015 13:00 UTC

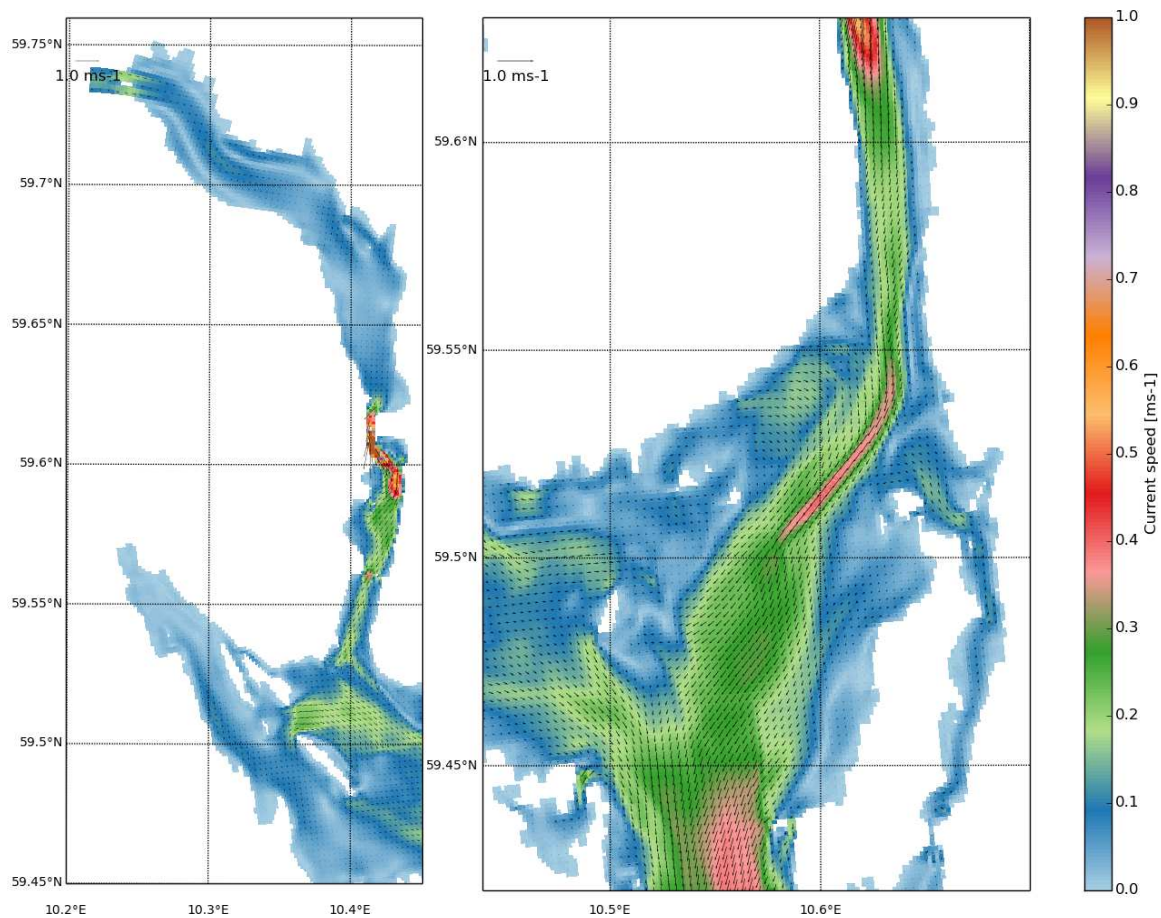


Figure 17: As Figure 15, but for the Drømmensfjord (left) and southern part of the Drøbak Sound and Breiangen area. Note the swift currents through narrow and shallow sound in the Svelvik area.

the narrow sounds, straits and other openings between islands.

Finally the major outflow is emptied into Skagerrak as the flow is getting close to the southern border of the FjordOs CL model domain. Due to the cyclonic motion in the Skagerrak the outflowing water is guided westward and flows inside of Store Færder to join the westward flowing current in the Skagerrak.

In summary the circulation pattern in upper water masses in the Oslofjord on March 23, 2015 is one of strong outflow that more or less is guided by the topography and hence meanders as it flows southward. In addition to this general flow the circulation pattern reveals detailed currents flowing through the many straits, narrow sounds and opening between islands. The latter is only made possible by the high resolution offered by the new FjordOs CL model.

Current at 2 m depth - 27-03-2015 13:00 UTC

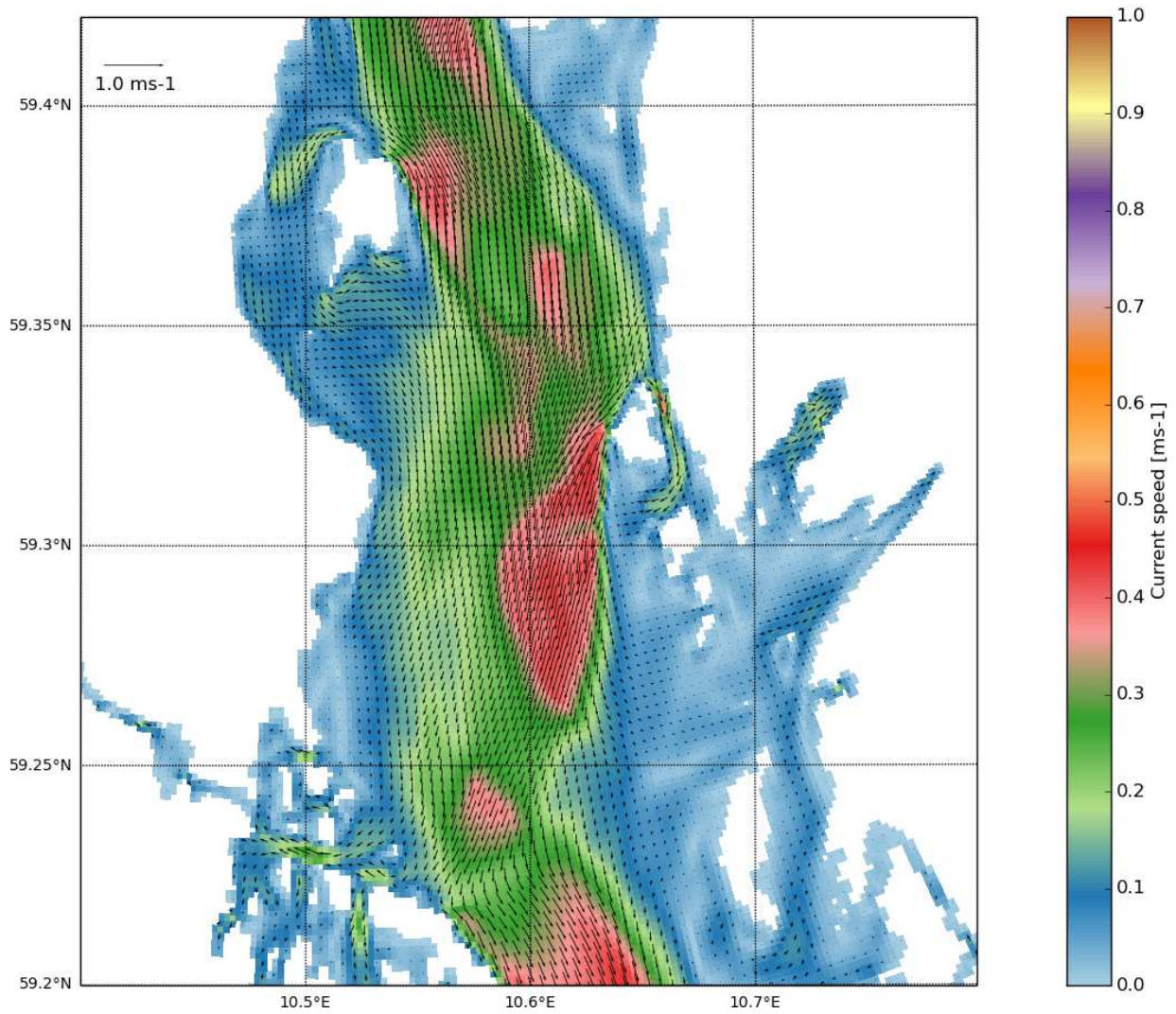


Figure 18: As Figure 15, but for the area between the Bastøy, Rauer and Bolærne islands.

Current at 2 m depth - 27-03-2015 13:00 UTC

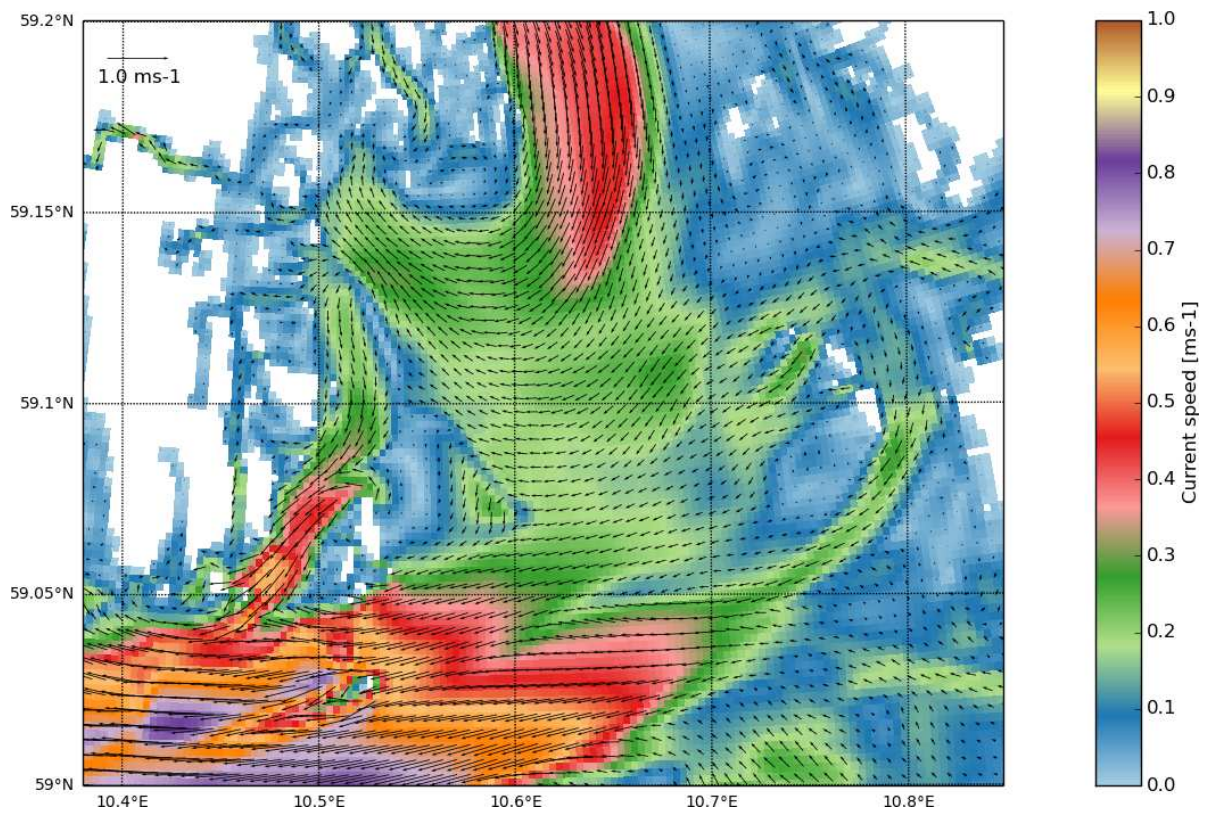


Figure 19: As Figure 15, but for the area around the Færder lighthouse.

5.2 Hydrography and sea level

It is also interesting to note the rich detail in the salinity and temperature patterns only made possible due to the high resolution of FjordOs CL model as revealed by Figures 20 and 21). Nevertheless the most striking feature to be observed is the impact of the rivers. In particular this is evident looking at the salinity distribution (Figure 20). In March the river discharge is starting to peak and hence increasing the freshwater content in the upper water masses of the fjord and in particular close to their mouths. This is particularly evident for the two major rivers Glomma and Drammenselva, but also clearly visible regarding Numedalslågen and Aulivassdraget (Tønsberg). At these locations the temperature is somewhat increased, in particular in the Drammensfjord, in comparison to the rest of the fjord. We believe this is due to entrainment of warm water from below due to the swift currents created there.

Regarding the water level at March 23, 2015 (Figure 22) we observe that this date is one of high sea level in the inner parts with lower sea levels as we proceed southwards. This is in line with the strong outflow described in Section 5.1 above.

Sea surface salinity - 27-03-2015 13:00 UTC

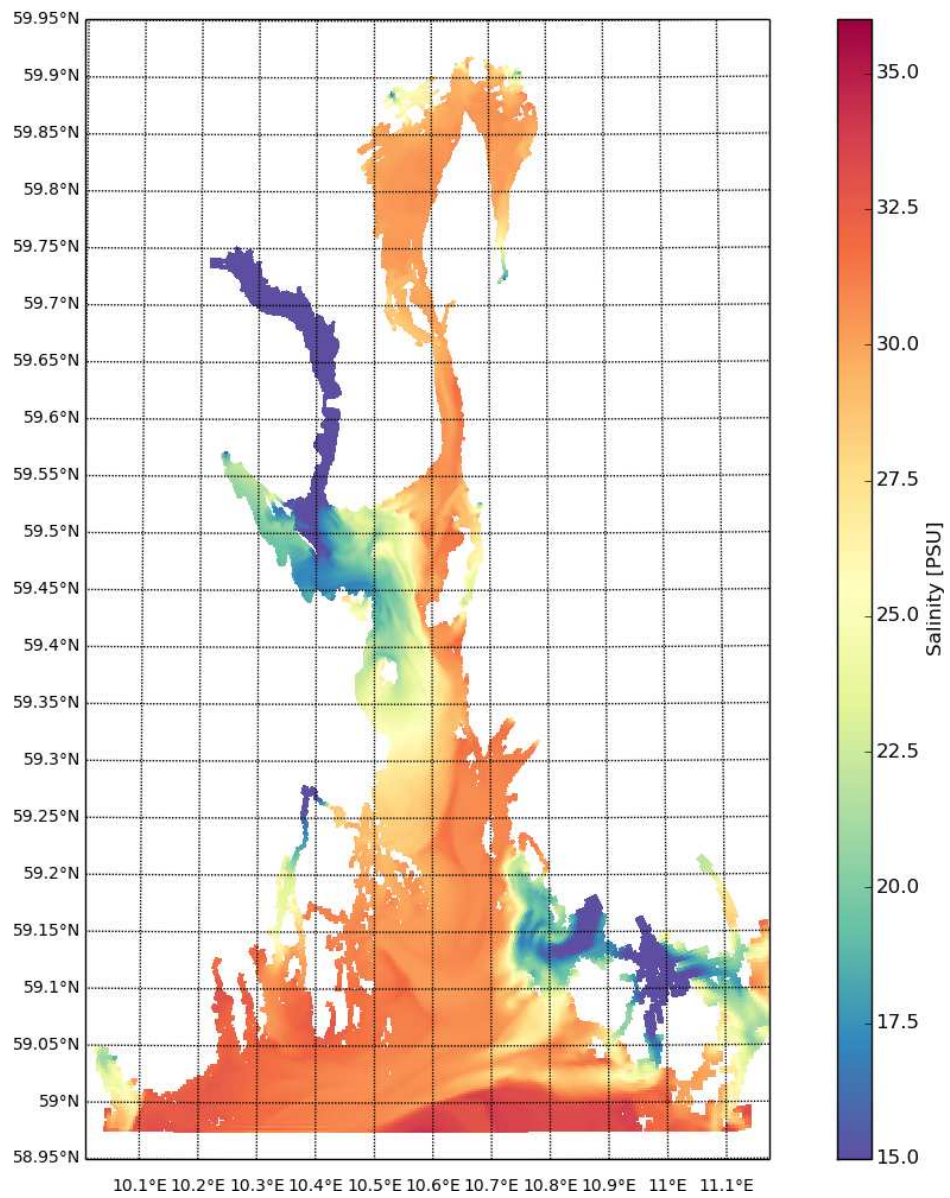


Figure 20: As Figure 21, but for sea surface salinity (SSS).

Sea surface temperature - 27-03-2015 13:00 UTC

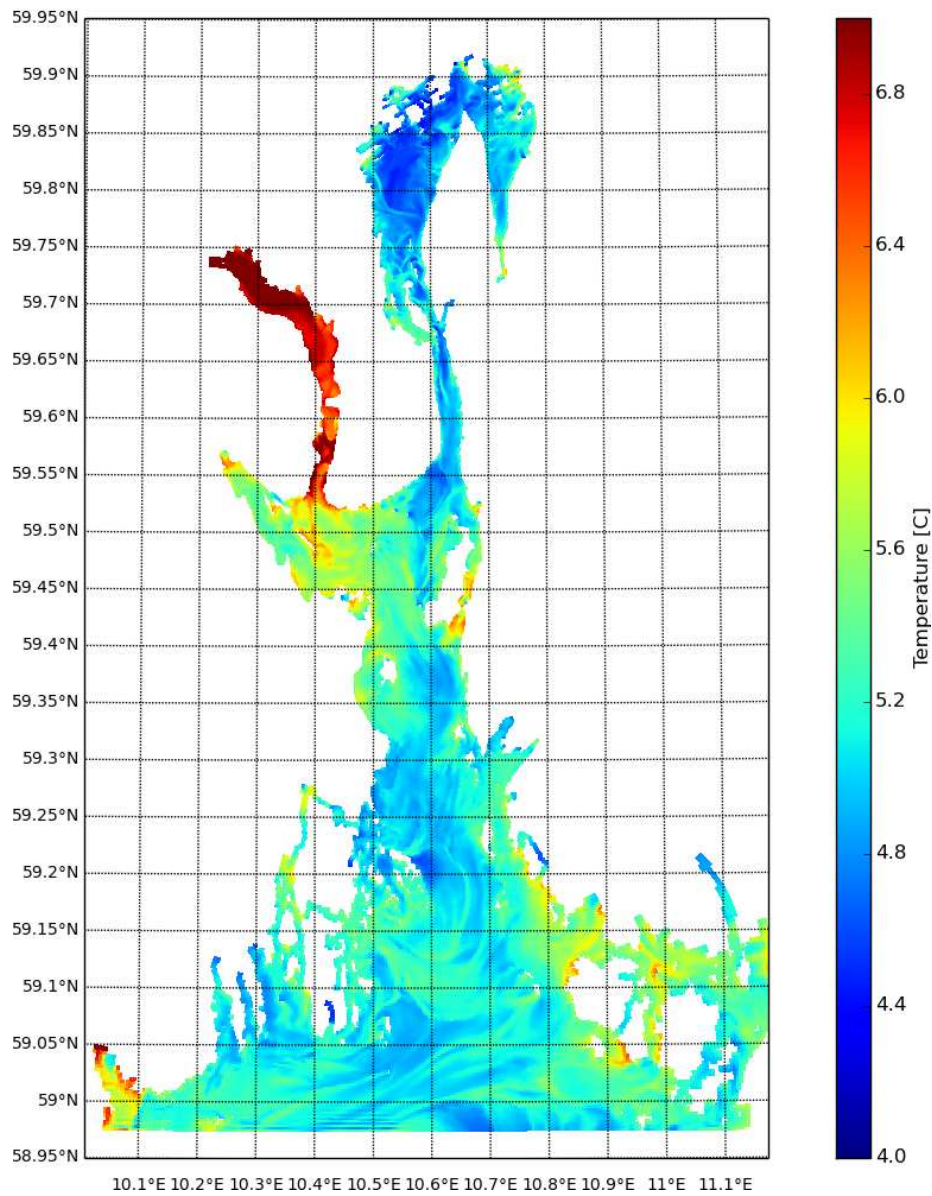


Figure 21: Sea surface temperature (SST) for the entire model domain of the FjordOs model. Note the high SST in the Drammensfjorden area. We believe this is most likely caused by the entrainment (mixing) of warmer water from below. This warm water is probably left from imperfect initial conditions.

Sea surface height - 27-03-2015 13:00 UTC

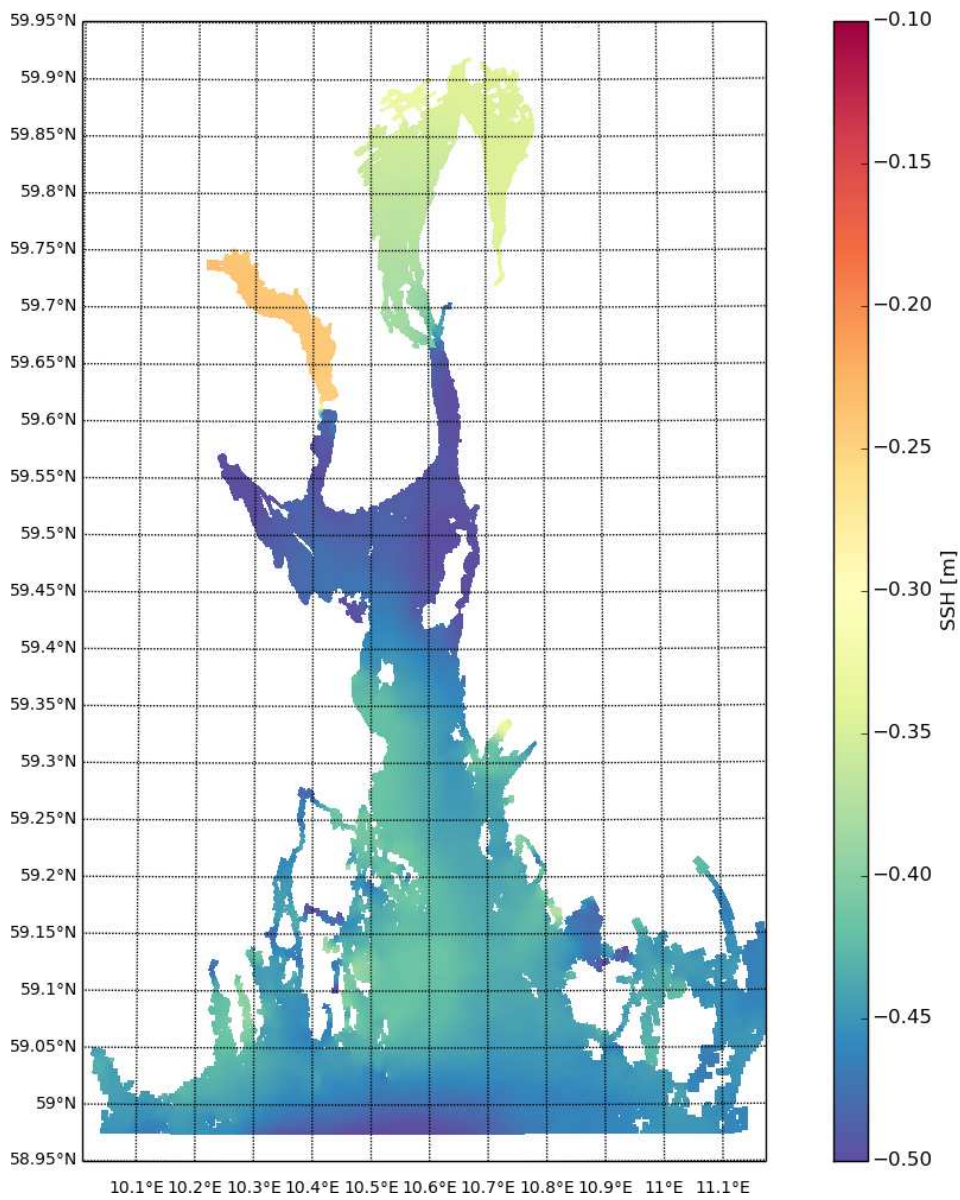


Figure 22: As for figure 21, but for sea surface height (SSH).

6 Summary and final remarks

A documentation of a new Oslofjord model is provided. The new Oslofjord model, named FjordOs CL, is based on the publically available ocean model ROMS (*Shchepetkin and McWilliams, 2005, 2009; Haidvogel et al., 2008*), and is developed as part of the project FjordOs. FjordOs CL exploits the curvilinear option in ROMS to minimize the number of “dry” grid points at the expense of increasing the number of “wet” grid points. Thereby the grid resolution is enhanced and varies in space. In fact the FjordOs CL mesh size varies from about 50 m in the Drøbak area to about 300 m at its southern border.

To satisfy ourselves that the model works technically, is viable and produces results that are in line with our knowledge of the circulation in the fjord, we have run several test cases. Above we have shown examples of results from a hindcast case initiated on April 1, 2014 and run through December 31, 2015. A thorough validation of the results from this hindcast will be reported in a separate report.

In summary the results shown provides insight into the necessity of resolving the Oslofjord’s irregular coastline geography, that is, the fjord’s many small islands, narrow sounds and straits, and its topography, that is, deep basins and shallow areas. Thus the new model provides a basis for developing an operation Oslofjord model once well identified and validated.

Acknowledgements

The present research and development is mostly funded by the the regional research funds Oslofjordfondet (Research grant no. 226022). We gratefully acknowledge the support. Smaller contributions from MET Norway, NIVA, HSN, Kystverket and Exxon are also appreciated. We would also like to thank Kai H. Christensen, Ann Kristin Sperrevik, Yvonne Gusdal and Arne Melsom, all from MET Norway, for many helpful discussions and suggestions.

References

- Albretsen, J., A. K. Sperrevik, A. Staalstrøm, A. D. Sandvik, F. Vikebø, and L. C. Asplin (2011), Norkyst-800 Report No. 1: User manual and technical descriptions, *Tech. Rep. Fisken og Havet 2/2011*, Institute of Marine Research, Pb. 1870 Nordnes, N-5817 Bergen, Norway.
- Beckmann, A., and D. B. Haidvogel (1993), Numerical simulation of flow around a tall isolated seamount. Part I: Problem formulation and model accuracy, *J. Phys. Oceanogr.*, 23, 1736–1753, doi:10.1175/1520-0485(1993)023<1736:NSOFAA>2.0.CO;2.
- Beldring, S., K. Engeland, L. A. Roald, N. R. Sælthun, and A. Voksø (2003), Estimation of parameters in a distributed precipitation-runoff model for Norway, *Hydrology and Earth System Sciences Discussions*, 7(3), 304–316.
- Egbert, G. D., and S. Y. Erofeeva (2002), Efficient inverse modeling of barotropic ocean tides, *J. Atmos. Oceanic Tech.*, 19(2), 183–204, doi:10.1175/1520-0426(2002)019<0183:EIMOBO>2.0.CO;2.
- Haidvogel, D. B., H. Arango, P. W. Budgell, B. D. Cornuelle, E. Curchitser, E. D. Lorenzo, K. Fennel, W. R. Geyer, A. J. Hermann, L. Lanerolle, J. Levin, J. C. McWilliams, A. J. Miller, A. M. Moore, T. M. Powell, A. F. Shchepetkin, C. R. Sherwood, R. P. Signell, J. C. Warner, and J. Wilkin (2008), Ocean forecasting in terrain-following coordinates: Formulation and skill assessment of the Regional Ocean Modeling System, *J. Comput. Phys.*, 227(7), 3595–3624, doi: <http://dx.doi.org/10.1016/j.jcp.2007.06.016>.
- Haney, R. L. (1991), On the pressure gradient force over steep topography in sigma coordinate ocean models, *J. Phys. Oceanogr.*, 21, 610–619.
- Hjelmervik, K. B., A. Staalstrøm, and S. E. Nordby (2014), Simulert tidevann i oslofjorden. tre forskjellige utforminger av havneområdet i Moss, *Technical Report L.NR. 6717-2014*, Norwegian Institute for Water Research, NIVA, Gaustadalléen 21, NO-0349 Oslo, Norway.
- Hjelmervik, K. B., N. M. Kristensen, A. Staalstrøm, and L. P. Røed (2016), Evaluation of the FjordOs CL model, *Technical Report in preparation*, Norwegian Meteorological Institute, MET Norway, P.O.Box 43 Blindern, NO-0313 Oslo, Norway.

- Marchesiello, P., J. C. McWilliams, and A. F. Shchepetkin (2001), Open boundary conditions for long-term integration of regional ocean models, *Ocean Modell.*, 3, 1–20, doi:10.1016/S1463-5003(00)00013-5.
- Milliman, J. D., and K. L. Farnsworth (2011), *River discharge to the coastal ocean: a global synthesis*, Cambridge University Press.
- Müller, M., M. Homleid, K.-I. Ivarsson, M. A. Køltzow, M. Lindskog, U. Andrae, T. Aspelien, D. Bjørge, P. Dahlgren, J. Kristiansen, R. Randriamampianina, M. Ridal, and O. Vignes (2015), AROME-MetCoOp: A Nordic convective scale operational weather prediction model, *Submitted*, -, -.
- Pawlowicz, R., B. Beardsley, and S. Lentz (2002), Classical tidal harmonic analysis including error estimates in MATLAB using T_TIDE, *Computers and Geosciences*, 28(8), 929–937.
- Røed, L. P., and J. Debernard (2004), Description of an integrated flux and sea-ice model suitable for coupling to an ocean and atmosphere model, *met.no Report 4/2004*, Norwegian Meteorological Institute, P.O. Box 43 Blindern, 0313 Oslo, Norway, [Available at http://met.no/Forskning/Publikasjoner/MET_report/2004/filestore/004_2004.pdf].
- Shchepetkin, A. F., and J. C. McWilliams (2003), A method for computing horizontal pressure-gradient force in an oceanic model with a nonaligned vertical coordinate, *J. Geophys. Res.*, 108, 3090, doi:10.1029/2001JC001047.
- Shchepetkin, A. F., and J. C. McWilliams (2005), The Regional Ocean Modeling System (ROMS): A split-explicit, free-surface, topography-following coordinate ocean model, *Ocean Modelling*, 9, 347–404.
- Shchepetkin, A. F., and J. C. McWilliams (2009), Correction and commentary for "Ocean forecasting in terrain-following coordinates: Formulation and skill assessment of the regional ocean modeling system" by Haidvogel et al., *J. Comp. Phys.* 227, pp. 3595-3624, *J. Comp. Phys.*, 228(24), 8985 – 9000, doi:10.1016/j.jcp.2009.09.002.
- Skarbøvik, E., P. Stålnacke, J. R. Selvik, P. A. Aakerøy, T. Høgåsen, and Ø. Kaste (2011), Elvetilførselsprogrammet (RID)-20 års overvåking av tilførsler til norske kystområder (1990-2009), *Tech. rep.*, Norsk institutt for vannforskning.

Song, T., and D. Haidvogel (1994), A semi-implicit ocean circulation model using a generalized topography-following coordinate system, *J. Comput. Phys.*, *115*, 228–244.

Umlauf, L., and H. Burchard (2003), A generic length-scale equation for geophysical turbulence models, *J. Marine Res.*, *61*, 235–265.